were very similar to those of α-syn deposited in the brains of patients with α-synucleinopathies, including PD and DLB.

Because the idea has been gaining ground that transient oligomers, rather than mature fibrils, are responsible for cytotoxicity, we examined whether soluble oligomers could be introduced into cells in the same manner as fibril seeds by means of LA treatment and whether they could function as seeds for intracellular α-syn aggregate formation. As shown in Fig. 4, *A* and *B*, we purified stable α-syn oligomers from recombinant α-syn treated with exifone, an inhibitor of *in vitro* α-syn aggregation, which is thought to inhibit filament formation of α-syn by stabilizing SDS-resistant soluble oligomers (22, 23). Then cells expressing α-syn or mock plasmid were treated with a mixture of the oligomer fraction (5 μg) and LA and incubated for 3 days. Immunoblot analyses of lysates of these cells did not detect any SDS-resistant soluble oligomeric α-syn, and the levels of phosphorylated α-syn in the Sarkosyl-soluble and -insoluble fractions showed no increase (Fig. 4, *C* and *D*). On the other hand, we observed phosphorylated and deposited α-syn in the Sarkosyl-soluble and -insoluble fractions in cells expressing α-syn treated with Seed αS (Fig. 4, *C* and *D*). These results showed that SDS-resistant soluble oligomer of α-syn could not be introduced into cultured cells in the same manner as monomeric α-syn and/or could not function as seeds for intracellular α-syn aggregation.

*Mutagenic Analysis of Nucleation-dependent Assembly of α-Syn*—To investigate further the nucleation-dependent polymerization of α-syn, we analyzed the polymerization of α-syn mutated or truncated at various residues or subdomains that are believed to be crucial for its aggregation. Overexpression of A53T familial Parkinson mutant α-syn, which is readily fibrillogenic *in vitro*, in the presence of Seed αS moderately increased the accumulation and phosphorylation of α-syn in the Sarkosyl-soluble and insolu-

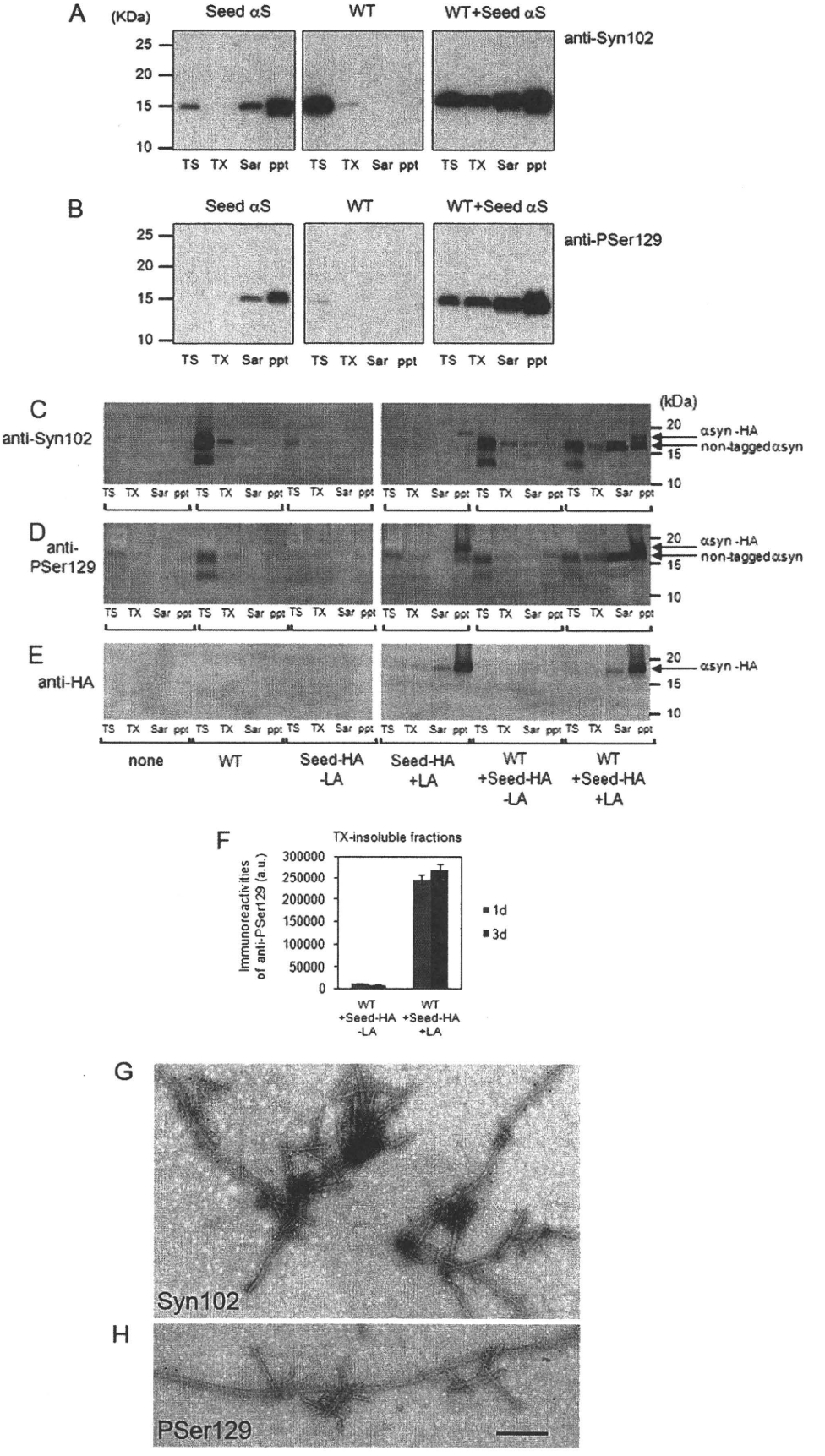

ble fractions compared with those in cells with wild-type α-syn expression and Seed αS (Fig. 5, *A* and *B*). In contrast, overexpression of Δ11 mutant α-syn, an assembly-incompetent mutant lacking residues 73–83, which have been shown to be essential for fibril formation of α-syn (24), elicited neither deposition nor phosphorylation of α-syn. We next introduced α-syn into SH-SY5Y cells expressing S129A mutant α-syn and observed slightly lower levels of Sarkosyl-insoluble α-syn compared with those in cells with wild-type α-syn expression and Seed αS. However, the frequency of inclusion bodies observed in seed-transduced cells expressing S129A was similar to that in seed-transfected cells expressing wild-type α-syn (data not shown), suggesting that phosphorylation at $Ser^{129}$ is not required for the nucleation-dependent polymerization of α-syn within cells.

*Nucleation-dependent Intracellular Polymerization of α-Syn Elicits Neurotoxicity and Cell Death*—SH-SY5Y cells overexpressing α-syn started to show marked clumping suggestive of cellular degeneration and death by ~48 h after introduction of seeds (Fig. 6*B*). Quantitative analysis of cell death by a lactate dehydrogenase (LDH) release assay at 72 h after introduction of Seed αS showed that cells overexpressing wild-type, A30P, A53T, or S129A α-syn released ~30% of total LDH from total cell lysate, whereas only ~12% of LDH was released from cells expressing Δ11 mutant α-syn, which lacks polymerization ability. In control cells transfected with empty vector or pcDNA3-α-syn followed by treatment with Lipofectamine without seeds, only ~7% of LDH was released (Fig. 6*C*). These results suggest a close correlation between the seed-dependent aggregation of α-syn and cell death. However, the dying cells transfected with fibrillization-competent α-syn and seeds did not show typical morphological changes of apoptosis (*e.g.* nuclear fragmentation, positive TUNEL staining (supplemental Fig. S4*A*), or activation of caspase-3 (supplemental Fig. S4*B*)), suggesting that they did not undergo typical apoptotic cell death, despite a previous report that exposure to neuron-derived extracellular α-syn may cause apoptosis (25).

*Impairment of Proteasome Activity in Cells with Intracellular Aggregates of α-Syn*—Because α-syn is ubiquitinated in the brains of patients with α-synucleinopathies (26) and inhibition of ubiquitin-proteasome systems by aggregates of proteins with expanded polyglutamine tracts has been reported (27), we analyzed the ubiquitination state of cellular proteins in α-syn aggregate-forming cells and compared the pattern with that in cells treated with a proteasome inhibitor, MG132. A Sarkosyl-soluble fraction of seed-transduced cells expressing wild-type α-syn and harboring abundant inclusions showed increased levels of ubiquitin-positive staining, which was similar in pattern to that observed in cells treated with MG132 (Fig. 6*D*). Because this pattern suggested an impairment of the ubiquitin-proteasome system, we directly analyzed the proteasome activity of α-syn inclusion-forming cells using a specific fluorescent peptide substrate, benzyloxycarbonyl-Leu-Leu-Glu-7-amido-4-methylcoumarin, that emits fluorescence following proteasomal digestion and confirmed that proteasome activity was significantly reduced in these cells as well as in cells treated with 20 μM MG132 for 4 h (Fig. 6*E*). We further examined the suppression of proteasome activity using CL1, a short degron that has been reported to be an effective proteasome degradation signal (28) and whose fusion protein with green fluorescent protein (GFP-CL1) has been used as a reporter for inhibition of proteasomal activity by intracellular polyglutamine aggregates (27) and intracellular α-syn (19). To examine if intracellular α-syn inclusions affected proteasomal activity, SH-SY5Y cells were transfected with both wild-type α-syn and GFP-CL1, followed by the introduction of Seed αS. Fluorescent signals of GFP were scarcely detected in control cells transfected with GFP-CL1 alone (Fig. 6*F*, *none*) but were markedly increased upon treatment with proteasome inhibitor MG132 (Fig. 6*F*, *MG132*), confirming that GFP-CL1 was effectively degraded by proteasome. Strikingly elevated GFP signals were detected in cells forming α-syn inclusions (Fig. 6*F*, *WT + Seed αS*) compared with those in control cells (Fig. 6*F*, *none* or *WT*), and GFP-CL1 and deposits of phosphorylated α-syn were co-localized within these cells (*arrowheads*). These results strongly suggest that proteasome activity is impaired in cells harboring α-syn inclusions elicited by the introduction of Seed αS.

*Small Molecular Inhibitors of Amyloid Filament Formation Protect against Cell Death Induced by Seed-dependent α-Syn Polymerization*—We have previously shown that several classes of small molecular compounds inhibit amyloid filament formation of α-syn, Tau, and Aβ *in vitro* (17, 23). These observations prompted us to test whether these inhibitors exert a protective effect against death of SH-SY5Y cells mediated by the nucleation-dependent polymerization of α-syn. Fig. 7*A* shows the effects of three polyphenol compounds, exifone, gossypetin, and quercetin, and a rifamycin compound, rifampicin, added to the culture media at a final concentration of 20 or 60 μM. Remarkably, all of these compounds blocked cell death, with gossypetin being the most effective. Our previous *in vitro* studies elucidated that several polyphenols, including gossypetin and exifone, inhibit α-syn assembly and that SDS-stable, noncytotoxic soluble α-syn oligomers are formed in their presence (23), suggesting that such polyphenols may inhibit filament formation of α-syn by stabilizing soluble, prefibrillar intermediates. Gossypetin or exifone might suppress intracellular α-syn aggregate formation by stabilizing such soluble intermediates in cultured cells as well. Immunoblot analysis

FIGURE 3. **Immunoblot and immunoelectron microscopic analyses of intracellular α-syn aggregates in cultured cells.** *A* and *B*, immunoblot analysis of α-syn in cells treated with Seed αS alone (*Seed αS*), pcDNA3-α-syn alone (*WT*), or both WT and Seed αS (*WT + Seed αS*). Proteins were differentially extracted from the cells with Tris-HCl (*TS*), Triton X-100 (*TX*), and Sarkosyl (*Sar*), leaving the pellet (*ppt*). Blots were probed using anti-α-syn (Syn102) (*A*) and anti-$Ser(P)^{129}$ (*PSer129*) (*B*). *C–F*, immunoblot analysis of proteins differentially extracted from mock (none) or cells transfected with pcDNA3-α-syn (*WT*), cells transduced with Seed-HA with (*Seed-HA + LA*) or without LA treatment (*Seed-HA − LA*), and cells overexpressing α-syn treated with Seed-HA with (*WT + Seed-HA + LA*) or without LA treatment (*WT + Seed-HA − LA*). Immunoreactivity of phosphorylated α-syn in the Triton X-100-insoluble fraction was quantified using anti-$Ser(P)^{129}$, and the results are expressed as means ± S.E. ($n = 3$), as shown in *F*. a.u., arbitrary unit. *G* and *H*, immunoelectron microscopy of α-syn filaments extracted from transfected cells. SH-SY5Y cells were transfected with both pcDNA3-α-syn and Seed αS. Sarkosyl-insoluble fraction was prepared from the cells, and the filaments were immunolabeled with anti-Syn102 (*G*) or $Ser(P)^{129}$ (*H*) antibody. *Scale bar*, 200 nm. *1d* and *3d*, 1 and 3 days, respectively.

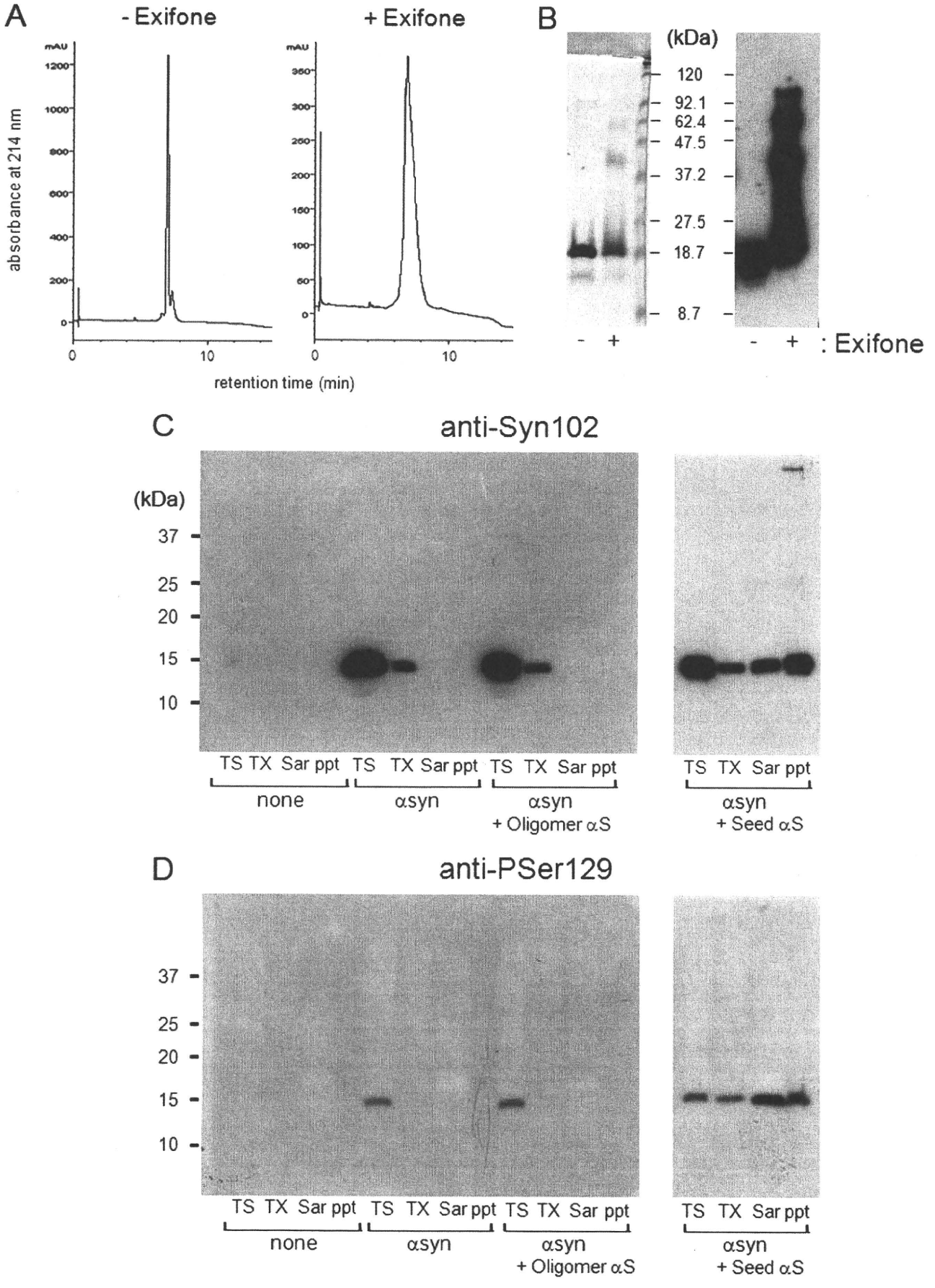
A
- Exifone
+ Exifone
mAU
absorbance at 214 nm
retention time (min)
B
(kDa)
120
92.1
62.4
47.5
37.2
27.5
18.7
8.7
- + : Exifone
C
anti-Syn102
(kDa)
37
25
20
15
10
TS TX Sar ppt
none
αsyn
αsyn + Oligomer αS
αsyn + Seed αS
D
anti-PSer129

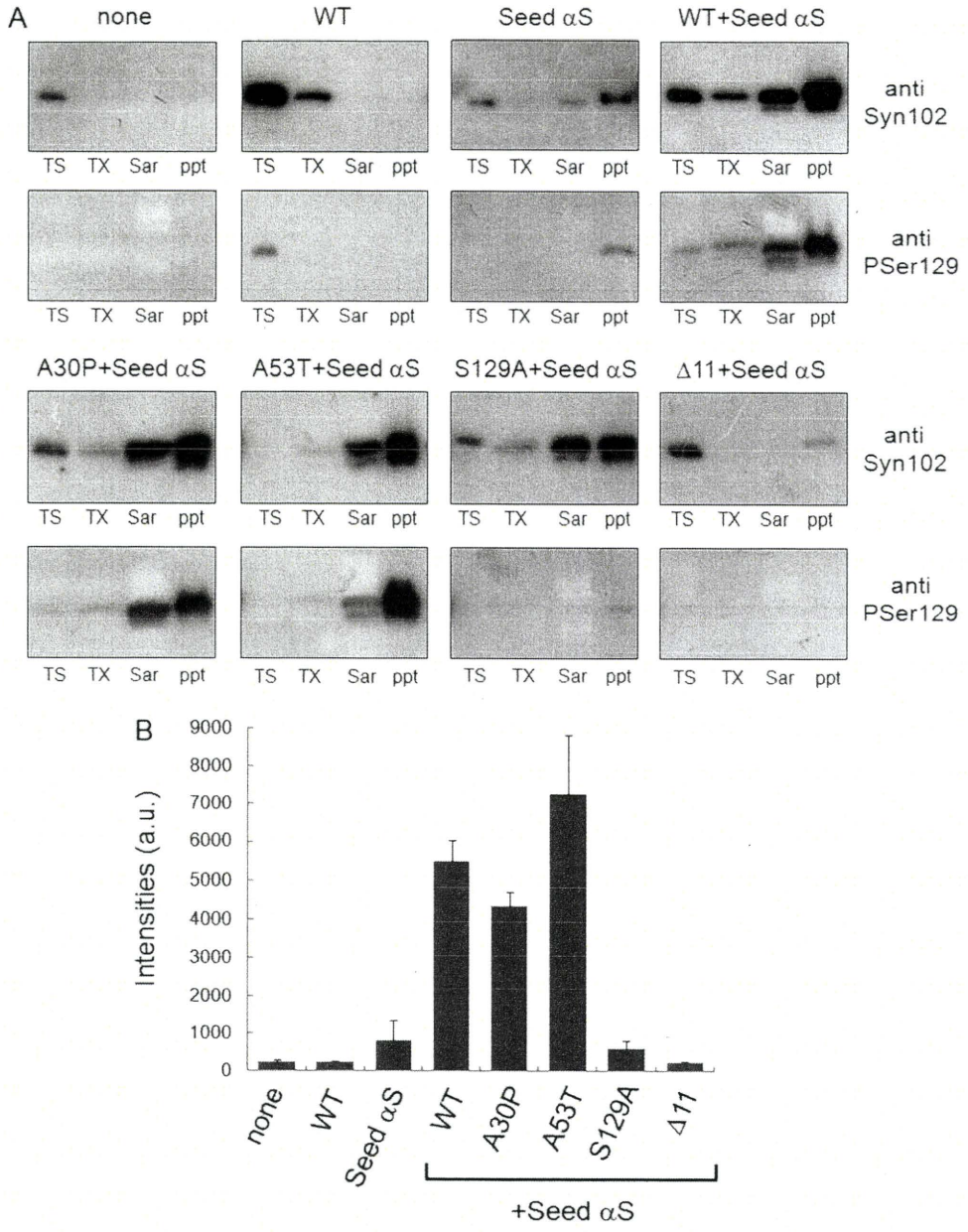


FIGURE 5. **Effects of α-syn mutations on intracellular deposition.** Immunoblot analysis of α-syn in cells transfected with pcDNA3-α-syn alone (*WT*), Seed αS alone (*Seed αS*), both WT and Seed αS (*WT + Seed αS*), and non-treated control cells (*none*). Cells overexpressing familial PD-linked A30P or A53T polymerization-deficient Δ11 mutant α-syn followed by transfection with Seed αS were also analyzed. Proteins were extracted differentially with Tris-HCl (*TS*), Triton-X (*TX*), and Sarkosyl (*Sar*), leaving the pellet (*ppt*), and immunoblotting was done with anti-Syn102 and Ser(P)$^{129}$ (*PSer129*). The Ser(P)$^{129}$-immunoreactive bands detected in Sarkosyl-soluble and -insoluble fractions from each cell type shown in *A* were quantified (*B*). The results are expressed as means +S.E. (*error bars*) ($n = 3$). a.u., arbitrary unit.

revealed that the levels of Sarkosyl-insoluble α-syn in cells transfected with both α-syn and seeds were reduced by treatment with exifone or gossypetin compared with those in untreated cells (Fig. 7*B*), supporting the notion that these compounds entered the cytoplasm and blocked cell death by suppressing the seed-dependent polymerization of α-syn.

*Cellular Models for Nucleation-dependent Polymerization of Tau*—Beside α-syn, Tau is another major pathogenic protein that is deposited in degenerating neurons or glial cells in various neurodegenerative diseases, and aggregation of distinct Tau isoforms has been found in different diseases (*i.e.* deposition of three-repeat Tau isoforms in Pick's disease, four-repeat Tau isoforms in progressive supranuclear palsy and corticobasal degeneration, and both three- and four-repeat Tau isoforms in AD). It is unknown why distinct Tau isoforms deposit in different diseases. Thus, we also tried to establish a cellular model of intracellular Tau aggregate formation by transduction of Tau fibril seeds into cultured cells. First, we confirmed that expression of 3R1N or 4R1N by itself induced phosphorylation of Ser$^{396}$, but no aggregated form was detected in detergent-insoluble fractions (Fig. 8 and supplemental Fig. S5). Next, we tested whether introduced Tau 4R1N or 3R1N fibril seed (Seed 4R1N or 3R1N, respectively) is detectable by immunoblot analysis using anti-T46, anti-HT7, or anti-Ser(P)$^{396}$ antibody. However, we could not detect any band in Triton X-100-insoluble fractions of cells treated with Seed Tau 4R1N or 3R1N in the presence of LA with any of these antibodies (data not shown). It seems likely that the efficiency of introduction of Tau 4R1N and 3R1N fibrils by LA treatment is very low, as compared with that of Seed αS. Then we checked whether treatment with recombinant Tau fibrils causes intracellular Tau aggregate formation in an LA-dependent manner. As shown in supplemental Fig. S5, LA treatment itself did not cause intracellular Tau deposition in cells expressing Tau 4R1N without Seed

FIGURE 4. **α-Syn oligomers were not introduced into cultured cells.** *A* and *B*, α-Syn oligomers were prepared as described under "Experimental Procedures." Oligomeric α-syn protein incubated with (47.8 μg of protein) or without exifone (30 μg of protein) was analyzed by reversed-phase HPLC (Aquapore RP-300 column) (*A*). These samples (0.2 μg of protein of each) were also analyzed by SDS-PAGE and immunoblotted with anti-Syn102 (*B*). *C* and *D*, cells were transfected with empty plasmid (*none*) or pcDNA3-αsyn (*αsyn*) and then treated with or without α-syn oligomer (*Oligomer αS, 5 μg*) or fibrils (*Seed αS, 2 μg*). After incubation for 3 days, cells were harvested, and immunoblot analyses were performed. Proteins differentially extracted from the cells with Tris-HCl (*TS*), Triton X-100 (*TX*), Sarkosyl (*Sar*), and the pellet (ppt) were probed using anti-Syn102 (*C*) and anti-Ser(P)$^{129}$ (*PSer129*) (*D*).

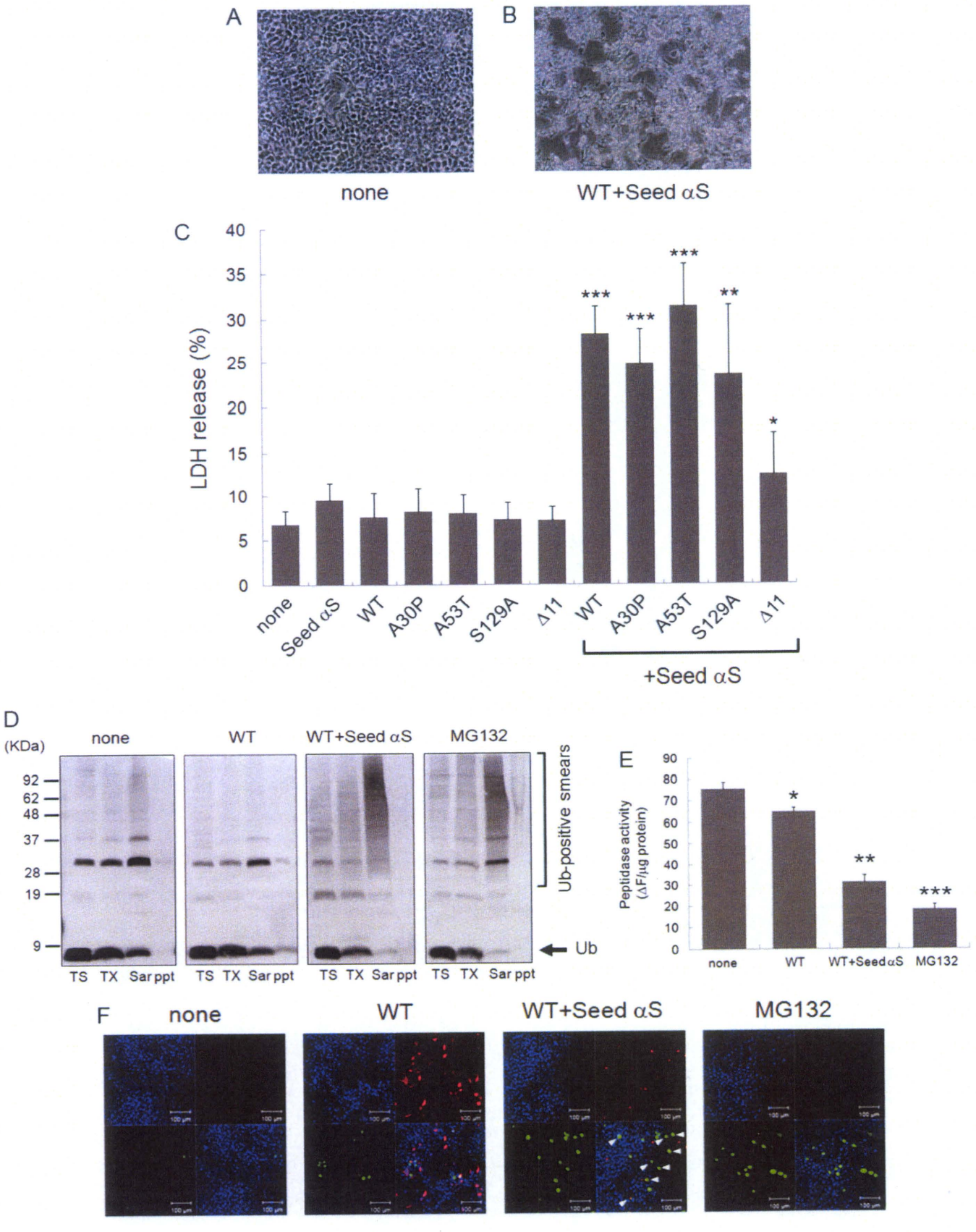
A
B
none
WT+Seed αS
C
LDH release (%)
40
35
30
25
20
15
10
5
0
***
***
***
**
*
none
Seed αS
WT
A30P
A53T
S129A
Δ11
WT
A30P
A53T
S129A
Δ11
+Seed αS
D
(KDa)
none
WT
WT+Seed αS
MG132
92
62
48
37
28
19
9
Ub-positive smears
Ub
TS TX Sar ppt
TS TX Sar ppt
TS TX Sar ppt
TS TX Sar ppt
E
Peptidase activity (ΔF/μg protein)
90
80
70
60
50
40
30
20
10
0
*
**
***
none
WT
WT+Seed αS
MG132
F
none
WT
WT+Seed αS
MG132

4R1N. Recombinant Tau 4R1N monomer in the presence of LA did not elicit the formation of intracellular Tau aggregates in these cells. On the other hand, when Seed 4R1N was added to cells expressing Tau 4R1N with LA, aggregated and phosphorylated Tau was detected in Sarkosyl-insoluble fractions by immunoblot analyses of these cell lysates using anti-HT7 or anti-Ser(P)$^{396}$ antibody (supplemental Fig. S5 and Fig. 8). In the case of intracellular Tau 3R1N aggregate formation, the results were similar to those in the experiments using Tau 4R1N described above (data not shown).

Intracellular aggregated four- or three-repeat Tau was also found to be detected with not only anti-Ser(P)$^{396}$ but also anti-AT100 antibody in the Sarkosyl-insoluble fraction (Fig. 8, *B* and *C*). Phosphorylated and deposited Tau was not found in the Triton X-100-insoluble fraction of Tau-expressing cells without Tau seed treatment or mock plasmid-expressing cells treated with Tau seed. In accordance with findings described earlier in this paper, these results suggested that soluble four- or three-repeat Tau expressed from the plasmid was accumulated into intracellular inclusions in the presence of small amounts of Seed 4R1N or 3R1N.

We also found that hyperphosphorylated and aggregated Tau was not detected in three-repeat Tau-expressing cells treated with Seed 4R1N (Fig. 8, *B* and *C*). On the other hand, the aggregated form of three-repeat Tau was detected in Triton X-100-insoluble fractions of three-repeat Tau-expressing cells treated with Seed 3R1N, and hyperphosphorylation at Ser$^{396}$ and Ser$^{212}$/Thr$^{214}$ was observed in fractionated samples of these cells, whereas no such bands were detected in four-repeat Tau-expressing cells treated with Seed 3R1N (Fig. 8, *B* and *C*). These results clearly showed that four-repeat Tau fibrils can be seeds for polymerization of four-repeat Tau, and three-repeat Tau fibrils can be seeds for polymerization of three-repeat Tau. Tau does not polymerize (cross-seed) in the presence of seeds of a different isoform. Similarly, no Tau aggregation was detected in Tau-expressing cells treated with α-syn fibril seeds (supplemental Fig. S3, *C* and *D*), and no α-syn aggregation was detected in α-syn-expressing cells transduced with Tau fibril seeds (data not shown). Furthermore, we observed anti-AT100 and anti-Ser(P)$^{396}$-positive Tau 4R1N or 3R1N filaments of ~15-nm width by negative stain electron microscopic analyses of Sarkosyl-insoluble fractions of cells transfected with both Tau plasmid and the seeds (Fig. 9, *A–D*).

Confocal microscopic analyses also showed that GFP-tagged Tau 4R1N (GFP-Tau 4R1N) is aggregated into round inclusions in the presence of Seed 4R1N together with LA (Fig. 8*E*). No inclusion-like structures were found in cells expressing GFP-Tau 4R1N (Fig. 8*D*) or in cells expressing GFP-Tau 4R1N after treatment with Seed 3R1N (data not shown). The ratio of the round aggregates to all GFP-positive transfectants was calculated to be 5.8% ± 0.8602 ($p = 0.0002$ by Student's *t* test against the value of cells expressing GFP-4R1N, $n = 5$). Significant cell death was not observed in cells containing intracellular 3R1N or 4R1N aggregates (data not shown). These results strongly suggest that proteins assemble easily into amyloid fibrils in the presence of amyloid seeds derived from the same protein but not a different protein.

## DISCUSSION

Nucleation-dependent protein polymerization occurs in many well characterized physiological processes (*e.g.* microtubule assembly and actin polymerization). It is also the mechanism of amyloid fibril formation in various pathological conditions and has been confirmed to occur *in vitro* for a wide variety of extracellular amyloids, such as Aβ peptides and prion proteins (12, 13) as well as intracellular proteins, such as α-syn and Tau (29, 30, 42). Both extra- and intracellular amyloids have been well studied *in vitro*, but much less is known about the mechanisms of assembly *in vivo*. Here we report a simple and effective method to introduce polymerization seeds into cells using Lipofectamine, a widely used transfection reagent. This method enabled us to evaluate the nucleation-dependent polymerization of α-synuclein and to establish a cellular model of the neurodegeneration seen in Parkinson disease.

Lipofectamine is a reagent widely used for the transfection of DNA into eukaryotic cells through the formation of liposomes of polycationic and neutral lipids in water, based on the principle of cell fusion. Various methods, including microinjection, the calcium phosphate method, the DEAE-dextran method, electroporation, and viral transfer, have been employed to introduce substances that are not normally incorporated into eukaryotic cells under physiological conditions. Microinjection is versatile but is not efficient in experiments involving large numbers of cells, and the traumatic damage to cells hampers evaluation of cytotoxic effects. Here, we have successfully employed lipofection to introduce protein aggregates as seeds

FIGURE 6. **Cell death caused by formation of intracellular α-syn inclusions.** *A* and *B*, phase-contrast microscopy of the control cells (*A*) and cells transfected with both pcDNA3-α-syn and Seed αS (*B*) 3 days after treatment with Seed αS (20× objective). *C*, the extent of cell death of transfected cells was quantified using an LDH release assay. Cells transfected with α-syn plasmid alone (WT, A30P, A53T, S129A, or Δ11) or with both wild-type or several mutants and Seed αS were incubated, and the cell death assay was performed 3 days thereafter. The results are expressed as means +S.E. (*error bars*) ($n = 5$). *, not significant; **, $p < 0.01$; ***, $p < 0.0005$ by Student's *t* test against the value of Seed αS. *D–F*, impairment of proteasome activity caused by intracellular aggregates of α-syn. *D*, immunoblot analysis of proteins sequentially extracted from non-treated cells (*none*) and cells transfected with wild-type α-syn plasmid alone (*WT*) or with both pcDNA3-α-syn and Seed αS (*WT + Seed αS*) and cells treated with 1 μM MG132 for 16 h (MG132) using anti-ubiquitin antibody. An *arrow* indicates monomeric ubiquitin. Polyubiquitinated proteins, reflecting impairment of the proteasome activity, are observed in the Sarkosyl-soluble fraction. *TS*, Tris-soluble; *TX*, 1% Triton X-100-soluble; *Sar*, 1% Sarkosyl-soluble; *ppt*, Sarkosyl-insoluble and SDS-soluble. *E*, peptide hydrolysis activity of proteasome. Cytosol fractions of non-treated control cells (*none*), cells transfected with wild-type α-syn plasmid alone (*WT*) or with WT and Seed αS (*WT + Seed αS*), and cells treated with 20 μM MG132 for 4 h (*MG132*) were prepared and assayed using benzyloxycarbonyl-Leu-Leu-Glu-7-amido-4-methylcoumarin as a substrate. The results are expressed as means +S.E. ($n = 3$). *, $p < 0.05$; **, $p < 0.01$; ***, $p < 0.0005$ by Student's *t* test against the value of none. *F*, proteasome activity in cells having intracellular aggregates of α-syn. SH-SY5Y cells transfected with both GFP-CL1 and WT were treated with Seed αS for 2 days, fixed, and stained with anti-Ser(P)$^{129}$. In the staining of cells transfected with wild-type α-syn plasmid alone (*WT*), anti-Syn102 was used. As a control, untreated or MG132-treated cells were also stained and analyzed. In untreated control cells, the fluorescence of GFP was poorly detected because GFP-CL1 could be degraded by proteasome in cells. In cells treated with MG132, fluorescence was markedly increased as compared with that in untreated cells because of the inhibition of proteasome activity by MG132. Co-localized images (*arrowheads*) with both increased intensities of GFP (*green*) and the fluorescence of anti-Ser(P)$^{129}$ (*red*) were detected in cells transfected with both WT and Seed αS (*WT + Seed αS*), indicating that the proteasome activity in these cells was inhibited.

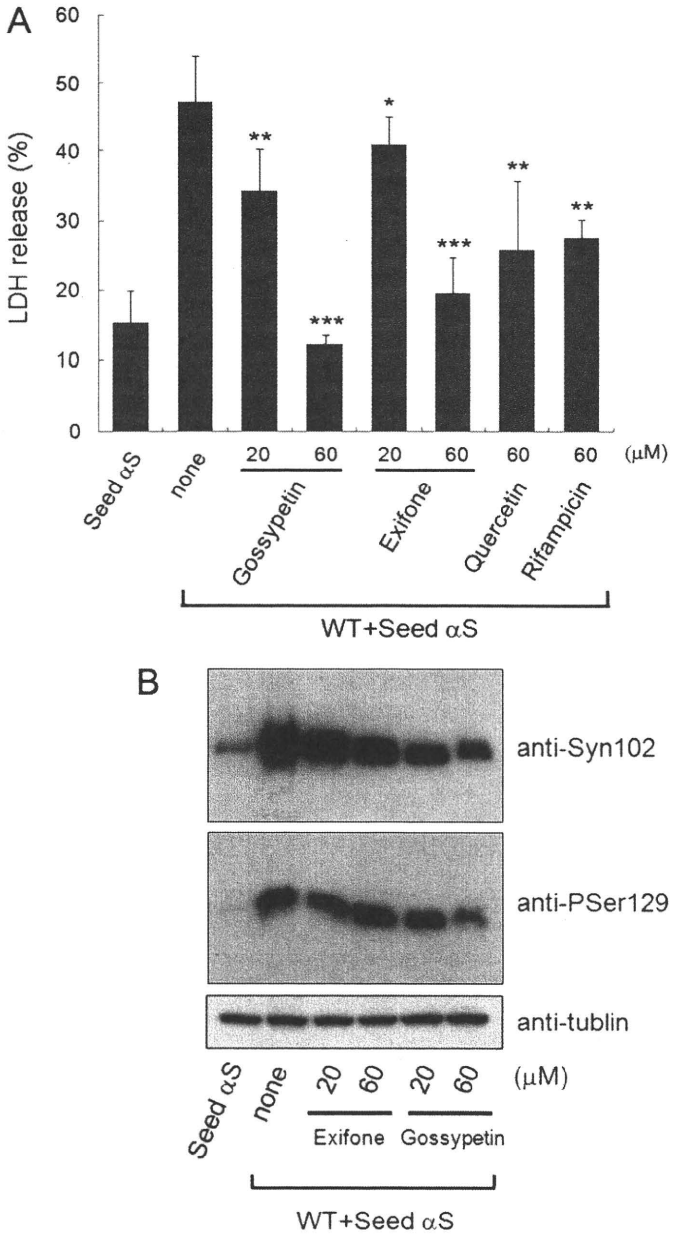


FIGURE 7. **Small molecular inhibitors of amyloid filament formation protect against cell death caused by intracellular α-syn aggregates.** *A*, the cell death of cells transfected with Seed αS and with both α-syn plasmid (*WT*) and Seed αS in the presence or absence of 20 or 60 μM gossypetin, 20 or 60 μM exifone, 60 μM quercetin, or 60 μM rifampicin was quantified by LDH release assay. The results are expressed as means ± S.E. (*error bars*) ($n = 4$). *, not significant; **, $p < 0.05$; ***, $p < 0.0005$ by Student's *t* test against the value of none. *B*, immunoblot analyses of the Sarkosyl-insoluble fraction prepared from cells transfected with Seed αS and with both WT and Seed αS in the absence or presence of exifone or gossypetin, with anti-Syn102 and anti-Ser(P)$^{129}$ (*PSer129*) antibodies. Doubly transfected cells were treated with 20 or 60 μM exifone or gossypetin 2 h after transfection of Seed αS and cultured for 3 days in the presence of polyphenols. Tubulin-α loading controls are also shown.

for amyloid fibril formation (patent pending for the United States (12/086124), the European Union (06834541.2), and Japan (2007-549210)). The reason why Lipofectamine could specifically incorporate Seed αS but not soluble α-syn into cells is unknown. However, one possibility is that aggregated α-syn with an ordered filamentous structure was preferentially bound to Lipofectamine and formed a complex that could be more effectively transported into cells compared with soluble α-syn, which has a random coil structure. In line with this idea, it has been reported that yeast prion fibrils can be introduced into yeast cells (31). Recently, Luk *et al.* (32) have also reported that α-syn monomers and fibrils but not oligomers were introduced into cells by Bioporter, a cationic-liposomal protein transduction reagent.

We confirmed the incorporation of insoluble α-syn seeds into cells by detecting phosphorylation of α-syn, as has been seen in intracellular aggregates of α-syn in various neurodegenerative conditions referred to as synucleinopathies. This suggests that Seed αS introduced into cells is a good target for phosphorylation at Ser$^{129}$. In contrast to our results, a recent report suggested that α-syn fibrils were not phosphorylated after internalization (32). It is possible that this specific phosphorylation represents an active attempt by cells to maintain the intracellular milieu by sequestering protein species that are harmful to cells. Notably, the phosphorylation of α-syn was dramatically increased when Seed αS was introduced into cells overexpressing soluble α-syn (Fig. 3 and supplemental Figs. S1*D* and S2). The possibility therefore arises that widespread propagation of hyperphosphorylation of α-syn throughout the cytoplasm reflects the activation of a certain kinase(s) associated with conversion of soluble α-syn into the fibrillar form in the presence of Seed αS. However, further investigation is needed to elucidate the importance of phosphorylation for protein aggregation.

The significance of intracellular and extracellular protein aggregates in neurodegeneration is still a matter of debate. The present results clearly show that nucleation-dependent polymerization of amyloid-like proteins is closely related to neuronal degeneration leading to cell death. According to the seeding theory, amyloid fibrils grow rapidly, without a time lag, when seeds are exposed to an amount of amyloidogenic soluble protein that exceeds the critical concentration. Our experiments with seed-transfected SH-SY5Y cells overexpressing α-syn clearly demonstrated that this is the case in the intracellular environment. We have unequivocally demonstrated that nucleation-dependent polymerization of amyloid-like fibrils can occur inside cells, and the intracellular filament formation elicits a variety of cellular reactions, including hyperphosphorylation and compromise of the ubiquitin proteasome system. We also showed that α-syn oligomers were not introduced into cells by LA and did not function as seeds for α-syn aggregate formation in cultured cells. It has been speculated that protein fibrils, not oligomers, are spread or transmitted in recently reported *in vivo* models (25, 33).

Our study also revealed that intracellular protein aggregation is highly dependent on the species of protein fibril seeds. This important finding may explain why only certain Tau isoforms are deposited in several tauopathies, including Pick disease, progressive supranuclear palsy, and corticobasal degeneration. In this study, α-syn fibrils were shown to be unable to seed intracellular Tau aggregation, which is consistent with neuropathological reports that deposited α-syn is not markedly colocalized with Tau aggregates. Our observations strongly support a seed-dependent mechanism for the formation of the intracellular protein aggregates.

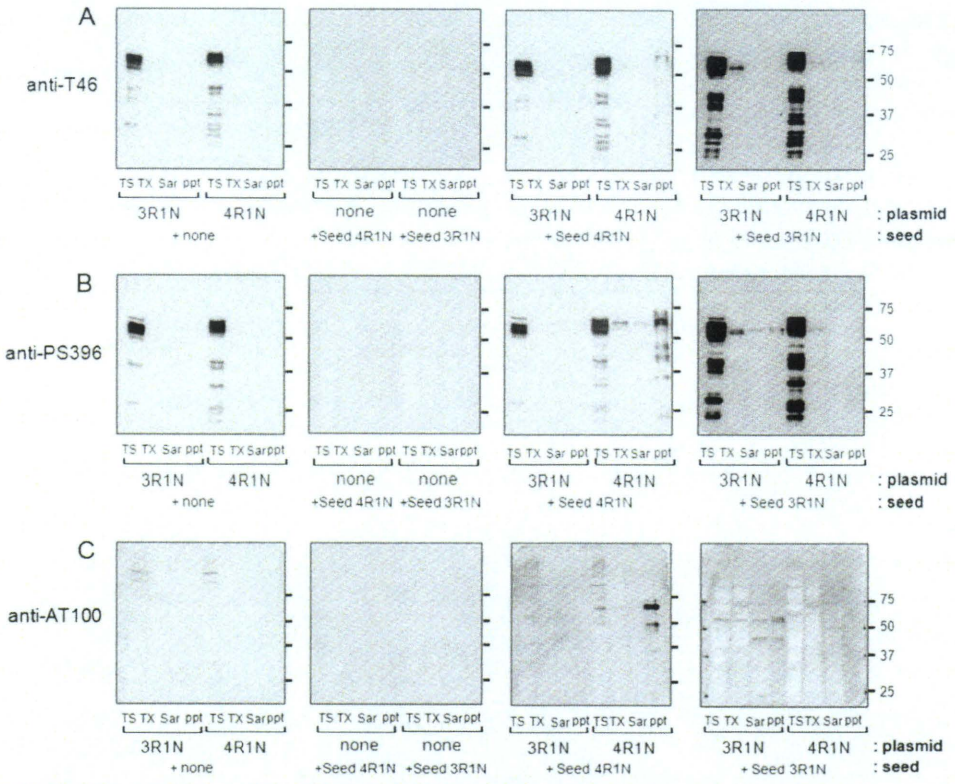


FIGURE 8. **Immunoblot analyses of intracellular Tau aggregates.** *A–C*, immunoblot analysis of Tau in cells treated with Tau fibrils alone (Seed 3R1N or Seed 4R1N), pcDNA3-Tau alone (3R1N or 4R1N), or both Seed Tau and pcDNA3-Tau. Tau proteins differentially extracted from the cells with Tris-HCl (*TS*), Triton X-100 (*TX*) and Sarkosyl (*Sar*), and the pellet (*ppt*) were probed with anti-T46 (*A*), anti-Ser(P)$^{396}$ (*PS396*) (*B*), and anti-AT100 (*C*).

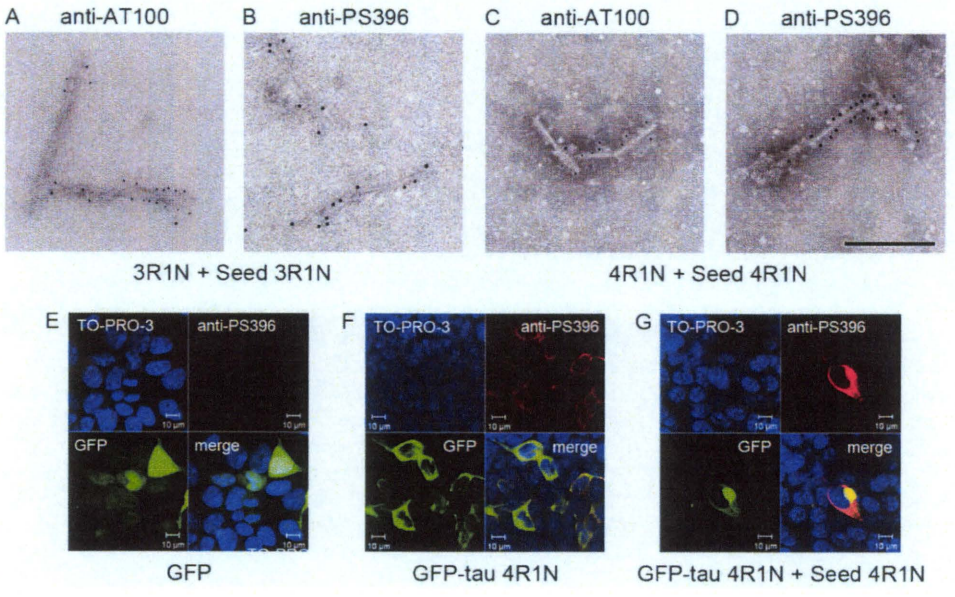


FIGURE 9. **Cellular models for intracellular Tau aggregation.** *A–D*, immunoelectron microscopy of Tau filaments extracted from transfected cells. SH-SY5Y cells were transfected with both pcDNA3-Tau 3R1N and Seed 3R1N (*A* and *B*) or pcDNA3-Tau 4R1N and Seed 4R1N (*C* and *D*). The Sarkosyl-insoluble fraction was prepared from the cells, and the filaments were immunolabeled with anti-AT100 (*A* and *C*) or anti-Ser(P)$^{396}$ (*PS396*) (*B* and *D*) antibody. *Scale bar*, 200 nm. *E–G*, confocal laser microscopic analyses of SH-SY5Y cells transfected with pEGFP empty vector (*E*), pEGFP-Tau 4R1N (*F*), and cells transfected with both pEGFP-Tau 4R1N and Seed 4R1N (*G*), immunostained with anti-Ser(P)$^{396}$ (*red*), and counterstained with TO-PRO-3 (*blue*). *Scale bars*, 10 μm.

Importantly, we showed that seed α-syn or Tau, an insoluble aggregate prepared from α-syn or Tau filaments, is effectively incorporated into cells by lipofection. This, in turn, suggests that high molecular weight protein aggregates or amyloid seeds shed from one cell may easily be propagated to others (*e.g.* neurons or glial cells) under pathological conditions (*e.g.* alteration in membrane permeability due to aging or virus infection, impairment of membrane function as a result of physical interaction with extracellular amyloid deposits, or abnormal membrane depolarization) that favor intracellular deposition of protein fibrils.

It remains to be clarified whether the incorporation of amyloid seeds into neurons or glial cells, as shown in this study, also occurs *in vivo*. However, some observations in AD or in transgenic animals support this possibility; apolipoprotein E (apoE) is involved in lipoprotein particle uptake mediated by cell surface receptors, and the E4 allele is the strongest genetic risk factor for AD. The apoE polypeptide has also been shown to bind Aβ (34), Tau (35), and the non-Aβ component of Alzheimer disease region of α-syn (36) and to be localized in amyloid plaques and neurofibrillary tangles in AD and prion plaques (37) in Creutzfeldt-Jakob disease. ApoE and low density lipoprotein receptor-related protein facilitate intraneuronal Aβ42 accumulation in transgenic mice (38). Furthermore, activation of both endocytic uptake and recycling of these proteins at a preclinical stage has been reported in sporadic AD and Down syndrome (39). Thus, it is strongly suggested that extracellular amyloid may be taken up into neurons by apoE and lipoprotein receptor-related protein-mediated endocytosis. Therefore, intracellular amyloid seeds composed of α-syn or Tau may also be incorporated into neurons by similar mechanisms when these seeds are released to the extracellular space after neuronal death.

It is well established that Tau protein starts to accumulate in the entorhinal region and spreads to the neocortices, closely correlating with the progression of AD (40). Similarly, accumulation of phosphorylated α-syn has been shown to start in vulnerable regions (*i.e.* limbic cortices) and to spread to the neocortices in PD or DLB. However, the mechanism of propagation of abnormal

protein deposition remains unknown. This study strongly supports a seed-dependent mechanism for the formation of the intracellular protein aggregates. In the context of our propagation hypothesis, it will be crucial to inhibit not only the production of intracellular amyloid seeds but also their spread into the extracellular space. Vaccination against the intracellular amyloid proteins, such as α-syn (41) or Tau may be an effective approach, together with inhibition of intracellular amyloid filament formation by small molecular inhibitors, for the therapy of these diseases.

*Acknowledgments—We thank Yoko Shimomura, Masami Masuda, and Ayaho Dan for technical assistance with immunoelectron microscopy and the preparation of recombinant Tau protein. We also thank Michel Goedert for helpful comments on the manuscript.*

## REFERENCES


1. Chiti, F., and Dobson, C. M. (2006) *Annu. Rev. Biochem.* **75,** 333–366
2. Goedert, M., Spillantini, M. G., and Davies, S. W. (1998) *Curr. Opin Neurobiol.* **8,** 619–632
3. Prusiner, S. B. (2001) *N. Engl. J. Med.* **344,** 1516–1526
4. Soto, C., Estrada, L., and Castilla, J. (2006) *Trends Biochem. Sci.* **31,** 150–155
5. Fujiwara, H., Hasegawa, M., Dohmae, N., Kawashima, A., Masliah, E., Goldberg, M. S., Shen, J., Takio, K., and Iwatsubo, T. (2002) *Nat. Cell Biol.* **4,** 160–164
6. Kirschner, D. A., Inouye, H., Duffy, L. K., Sinclair, A., Lind, M., and Selkoe, D. J. (1987) *Proc. Natl. Acad. Sci. U.S.A.* **84,** 6953–6957
7. Eanes, E. D., and Glenner, G. G. (1968) *J. Histochem. Cytochem.* **16,** 673–677
8. Nguyen, J. T., Inouye, H., Baldwin, M. A., Fletterick, R. J., Cohen, F. E., Prusiner, S. B., and Kirschner, D. A. (1995) *J. Mol. Biol.* **252,** 412–422
9. Serpell, L. C., Berriman, J., Jakes, R., Goedert, M., and Crowther, R. A. (2000) *Proc. Natl. Acad. Sci. U.S.A.* **97,** 4897–4902
10. Berriman, J., Serpell, L. C., Oberg, K. A., Fink, A. L., Goedert, M., and Crowther, R. A. (2003) *Proc. Natl. Acad. Sci. U.S.A.* **100,** 9034–9038
11. Perutz, M. F. (1999) *Trends Biochem. Sci.* **24,** 58–63
12. Harper, J. D., and Lansbury, P. T., Jr. (1997) *Annu. Rev. Biochem.* **66,** 385–407
13. Jarrett, J. T., and Lansbury, P. T., Jr. (1993) *Cell* **73,** 1055–1058
14. Jakes, R., Spillantini, M. G., and Goedert, M. (1994) *FEBS Lett.* **345,** 27–32
15. Nonaka, T., Iwatsubo, T., and Hasegawa, M. (2005) *Biochemistry* **44,** 361–368
16. Aoyagi, H., Hasegawa, M., and Tamaoka, A. (2007) *J. Biol. Chem.* **282,** 20309–20318
17. Taniguchi, S., Suzuki, N., Masuda, M., Hisanaga, S., Iwatsubo, T., Goedert, M., and Hasegawa, M. (2005) *J. Biol. Chem.* **280,** 7614–7623
18. Nonaka, T., Kametani, F., Arai, T., Akiyama, H., and Hasegawa, M. (2009) *Hum. Mol. Genet.* **18,** 3353–3364
19. Nonaka, T., and Hasegawa, M. (2009) *Biochemistry* **48,** 8014–8022
20. Sung, J. Y., Kim, J., Paik, S. R., Park, J. H., Ahn, Y. S., and Chung, K. C. (2001) *J. Biol. Chem.* **276,** 27441–27448
21. Spillantini, M. G., Crowther, R. A., Jakes, R., Hasegawa, M., and Goedert, M. (1998) *Proc. Natl. Acad. Sci. U.S.A.* **95,** 6469–6473
22. Conway, K. A., Rochet, J. C., Bieganski, R. M., and Lansbury, P. T., Jr. (2001) *Science* **294,** 1346–1349
23. Masuda, M., Suzuki, N., Taniguchi, S., Oikawa, T., Nonaka, T., Iwatsubo, T., Hisanaga, S., Goedert, M., and Hasegawa, M. (2006) *Biochemistry* **45,** 6085–6094
24. Giasson, B. I., Murray, I. V., Trojanowski, J. Q., and Lee, V. M. (2001) *J. Biol. Chem.* **276,** 2380–2386
25. Desplats, P., Lee, H. J., Bae, E. J., Patrick, C., Rockenstein, E., Crews, L., Spencer, B., Masliah, E., and Lee, S. J. (2009) *Proc. Natl. Acad. Sci. U.S.A.* **106,** 13010–13015
26. Hasegawa, M., Fujiwara, H., Nonaka, T., Wakabayashi, K., Takahashi, H., Lee, V. M., Trojanowski, J. Q., Mann, D., and Iwatsubo, T. (2002) *J. Biol. Chem.* **277,** 49071–49076
27. Bence, N. F., Sampat, R. M., and Kopito, R. R. (2001) *Science* **292,** 1552–1555
28. Gilon, T., Chomsky, O., and Kulka, R. G. (1998) *EMBO J.* **17,** 2759–2766
29. Friedhoff, P., von Bergen, M., Mandelkow, E. M., Davies, P., and Mandelkow, E. (1998) *Proc. Natl. Acad. Sci. U.S.A.* **95,** 15712–15717
30. Wood, S. J., Wypych, J., Steavenson, S., Louis, J. C., Citron, M., and Biere, A. L. (1999) *J. Biol. Chem.* **274,** 19509–19512
31. Tanaka, M., Chien, P., Yonekura, K., and Weissman, J. S. (2005) *Cell* **121,** 49–62
32. Luk, K. C., Song, C., O'Brien, P., Stieber, A., Branch, J. R., Brunden, K. R., Trojanowski, J. Q., and Lee, V. M. (2009) *Proc. Natl. Acad. Sci. U.S.A.* **106,** 20051–20056
33. Clavaguera, F., Bolmont, T., Crowther, R. A., Abramowski, D., Frank, S., Probst, A., Fraser, G., Stalder, A. K., Beibel, M., Staufenbiel, M., Jucker, M., Goedert, M., and Tolnay, M. (2009) *Nat. Cell Biol.* **11,** 909–913
34. Strittmatter, W. J., Saunders, A. M., Schmechel, D., Pericak-Vance, M., Enghild, J., Salvesen, G. S., and Roses, A. D. (1993) *Proc. Natl. Acad. Sci. U.S.A.* **90,** 1977–1981
35. Strittmatter, W. J., Saunders, A. M., Goedert, M., Weisgraber, K. H., Dong, L. M., Jakes, R., Huang, D. Y., Pericak-Vance, M., Schmechel, D., and Roses, A. D. (1994) *Proc. Natl. Acad. Sci. U.S.A.* **91,** 11183–11186
36. Olesen, O. F., Mikkelsen, J. D., Gerdes, C., and Jensen, P. H. (1997) *Brain Res. Mol. Brain Res.* **44,** 105–112
37. Namba, Y., Tomonaga, M., Kawasaki, H., Otomo, E., and Ikeda, K. (1991) *Brain Res.* **541,** 163–166
38. Zerbinatti, C. V., Wahrle, S. E., Kim, H., Cam, J. A., Bales, K., Paul, S. M., Holtzman, D. M., and Bu, G. (2006) *J. Biol. Chem.* **281,** 36180–36186
39. Cataldo, A. M., Peterhoff, C. M., Troncoso, J. C., Gomez-Isla, T., Hyman, B. T., and Nixon, R. A. (2000) *Am. J. Pathol.* **157,** 277–286
40. Braak, H., and Braak, E. (1991) *Acta Neuropathol.* **82,** 239–259
41. Masliah, E., Rockenstein, E., Adame, A., Alford, M., Crews, L., Hashimoto, M., Seubert, P., Lee, M., Goldstein, J., Chilcote, T., Games, D., and Schenk, D. (2005) *Neuron* **46,** 857–868
42. Yonetani, M., Nonaka, T., Masuda, M., Inukai, Y., Oikawa, T., Hisanaga, S. I., and Hasegawa, M. (2009) *J. Biol. Chem.* **284,** 7940–7950

Acta Neuropathol (2010) 120:789–801
DOI 10.1007/s00401-010-0731-9

ORIGINAL PAPER

# Effect of topographical distribution of α-synuclein pathology on TDP-43 accumulation in Lewy body disease

**Osamu Yokota · Yvonne Davidson · Tetsuaki Arai · Masato Hasegawa · Haruhiko Akiyama · Hideki Ishizu · Seishi Terada · Stephen Sikkink · Stuart Pickering-Brown · David M. A. Mann**

Received: 6 May 2010 / Revised: 19 July 2010 / Accepted: 20 July 2010 / Published online: 29 July 2010


**Abstract** It has been reported that the development of TDP-43 pathology in cases of Lewy body disease (LBD) might be associated with the severity of tau pathology. However, the impact of α-synuclein pathology on TDP-43 accumulation in LBD remains unclear. To clarify whether α-synuclein pathology has an effect on TDP-43 accumulation, independent of tau pathology, we examined by immunohistochemistry 56 cases of LBD using a phosphorylation-dependent TDP-43 antibody. The frequency of TDP-43 pathology in all LBD cases was 18% (10/56). In 37 LBD cases with no or low tau burden (LBD-Ltau; Braak NFT stages 0-II), the frequency of TDP-43 pathology was 19% (7/37). The frequency of TDP-43 pathology in diffuse neocortical type LBD-Ltau cases was 36% (4/11), which was higher than those in limbic and brain stem-predominant types (11–14%). The amygdala and entorhinal cortex were the most frequently affected sites of TDP-43 pathology in LBD-Ltau cases. In LBD-Ltau cases, the proportion of diffuse neocortical type LBD was higher in the TDP-43-positive cases, than that in TDP-43-negative cases (57 vs. 23%). In all LBD cases, α-synuclein pathology in the temporal cortex was significantly more severe in TDP-43-positive cases, and significantly correlated with the severity of TDP-43 pathology in the amygdala. In a multivariate model, the presence of severe α-synuclein pathology was significantly associated with the development of TDP-43 pathology independent of age at death and tau pathology. In the amygdala, TDP-43 was often colocalized with α-synuclein or tau. Given these findings, we suggest that α-synuclein pathology is associated with TDP-43 accumulation in LBD cases.

**Keywords** α-Synuclein · DLB · Lewy body disease · Tau · TDP-43

O. Yokota · Y. Davidson · D. M. A. Mann (✉)
Neurodegeneration and Mental Health Research Group, Faculty of Medical and Human Sciences, School of Community Based Medicine, Greater Manchester Neurosciences Centre, Hope Hospital, University of Manchester, Salford M6 8HD, UK
e-mail: david.mann@manchester.ac.uk

S. Sikkink · S. Pickering-Brown
Neurodegeneration and Mental Health Research Group, Faculty of Medical and Human Sciences, School of Community Based Medicine, A V Hill Building, University of Manchester, Oxford Rd, Manchester M13 9PL, UK

T. Arai · H. Akiyama
Department of Psychogeriatrics, Tokyo Institute of Psychiatry, 2-1-8 Kamikitazawa, Setagaya-ku, Tokyo 156-8585, Japan

M. Hasegawa
Department of Molecular Neurobiology, Tokyo Institute of Psychiatry, 2-1-8 Kamikitazawa, Setagaya-ku, Tokyo 156-8585, Japan

O. Yokota · H. Ishizu · S. Terada
Department of Neuropsychiatry, Okayama University Graduate School of Medicine, Dentistry and Pharmaceutical Sciences, 2-5-1 Shikata-cho, Okayama 700-8558, Japan

H. Ishizu
Zikei Institute of Psychiatry, 100-2, Urayasu-honcho, Okayama 702-8508, Japan

## Introduction

The transactivation-responsive DNA-binding protein of $M_r$ 43 kDa, TDP-43, is a major component of ubiquitin-positive and tau-negative inclusions in the frontotemporal cortex and motor neurons in frontotemporal lobar degeneration (FTLD-U) and in amyotrophic lateral sclerosis (ALS), and is considered to play an essential pathogenic

role in these diseases, now called TDP-43 proteinopathies [3, 6, 7, 29]. However, abnormal TDP-43 accumulations have been demonstrated in cases of Alzheimer's disease (AD) [1, 2, 15], ALS/parkinson–dementia complex of Guam (ALS/PDC of Guam) [9, 12], argyrophilic grain disease (AGD) [8], corticobasal degeneration (CBD) [32], and progressive supranuclear palsy (PSP) [34]. Additionally, some (but not all) studies have supported the possibility that the severity of tau pathology is associated with TDP-43 accumulation in AD [1, 2], AGD [8], and PSP [34].

A few studies have demonstrated a concurrent TDP-43 pathology in some cases with Lewy body disease (LBD), including ones with Parkinson's disease (PD), Parkinson's disease with dementia (PDD), and dementia with Lewy bodies (DLB). The reported frequencies of TDP-43 pathological changes in several LBD series ranged from 19 to 60% [2, 14, 28]. However, most LBD cases have variable degrees of AD-type pathology [11, 17, 21–23, 27, 30, 33]. Indeed, in the earliest (and largest) study that examined TDP-43 pathology in LBD, approximately 50% of 180 LBD cases had moderate to severe tau pathology, and a higher frequency of TDP-43 pathology was observed in cases with a more severe Braak NFT stage score [28]. In a recent study, about 70% of TDP-43-positive LBD cases had moderate to severe tau pathology (Braak NFT stages III–VI) [2]. Nonetheless, somewhat unexpectedly, it has never been examined whether the development of TDP-43 pathology in LBD is influenced by α-synuclein pathology, or can simply be explained by the effect of concurrent tau pathology. Higashi et al. [14] reported no significant difference in the severity of α-synuclein pathology between DLB cases with or without TDP-43 pathology, and AD cases with or without TDP-43 pathology. However, the number of subjects in the study was small (11 DLB cases including 5 TDP-43-positive cases, and 15 AD cases including 5 TDP-43-positive cases), and the influence of tau pathology was not compensated for.

The principal aim of this study was to investigate whether the presence of α-synuclein pathology is associated with TDP-43 accumulation in LBD. To address this, we revisited the frequency and distribution of TDP-43 pathology using a phosphorylation-dependent TDP-43 antibody in LBD cases with no or low tau burden (corresponding to Braak NFT stages 0–II [4]) (i.e., LBD-Ltau cases) and LBD cases with more severe tau burden (Braak NFT stages III–VI) (LBD-Htau cases). Secondly, we compared the severities of α-synuclein and tau pathologies between LBD cases with and without TDP-43 accumulation, and also examined the correlation between the severity of TDP-43 pathology and that of α-synuclein or tau pathology. Thirdly, we examined the frequencies of TDP-43 pathology in three subtypes of LBD (i.e., brain stem-predominant type, limbic type, and diffuse neocortical type [27]) concentrating especially on the LBD-Ltau cases, and asking whether the severity of α-synuclein pathology was independently associated with the development of TDP-43 pathology in all LBD cases using multivariate models. Finally, we performed double immunofluorescence labeling and biochemical examination in order to further understand the pathogenic mechanism underlying TDP-43 accumulation in LBD.

## Materials and methods

### Subjects

All of the available pathologically confirmed LBD cases ($n = 56$) in the UK Parkinson's Disease Society Tissue Bank, as well as pathologically normal controls ($n = 4$), were examined in this study. The clinical diagnosis in these cases was LBD (i.e., 29 cases of PD, 51.8%; 23 cases of PDD, 41.1%; and 4 cases of DLB, 7.1%). The clinical diagnosis of PDD was based on motor impairment preceding cognitive impairment by at least 1 year [27]. The most frequent pathological subtype of LBD in our series was limbic type (51.8%), followed by the diffuse neocortical type (30.4%) and lastly the brainstem-predominant type (17.9%). No cases having other degenerative diseases, such as PSP, CBD, and multiple system atrophy, were included in this study. The proportion of LBD cases with severe tau pathology in this series was low: 37 cases (66% of all LBD cases) had no or low tau burden corresponding to Braak NFT stages 0–II (i.e., were LBD-Ltau cases): 30 cases (53.6%) corresponded to Braak NFT stage II, six cases (10.7%) were Braak NFT stage I, and only one case completely lacked tau pathology (1.8%). The other 19 cases (34%) had a higher tau burden corresponding to Braak NFT stages III–VI (i.e., LBD-Htau cases): ten cases (17.9%) corresponded to Braak NFT stage III, four cases (7.1%) had stage IV, three cases (5.4%) had stage V, and two cases (3.6%) had stage VI. Thirty-eight cases (68% of all LBD cases) had various degrees of Aβ deposits in the hippocampus and/or temporal cortex. Argyrophilic grains were found in two LBD cases. All brains had been collected with Local Research Ethical Committee approval. Relevant clinical and pathological features for all 56 LBD cases are shown in Table 1.

### Immunohistochemistry

Paraffin sections were cut at 6 μm thickness, to include the amygdala, entorhinal cortex, hippocampus, and occipitotemporal cortex, from all LBD cases and immunostained with antibodies against phosphorylated TDP-43 (pAb

**Table 1** Clinical and pathological features in LBD cases with and without TDP-43 pathology

| | All | TDP-43-positive | TDP-43-negative | *P* value[a] |
|---|---|---|---|---|
| *N* (%) | 56 (100.0) | 10 (17.9) | 46 (82.1) | – |
| Male [*N* (%)] | 42 (75.0) | 8 (80.0) | 34 (73.9) | 1.000 |
| Age at onset [mean (SD)] | 62.8 (13.2) | 65.2 (11.0) | 62.3 (13.8) | 0.561 |
| Age at death [mean (SD)] | 76.9 (7.2) | 77.4 (6.7) | 76.8 (7.3) | 0.899 |
| Duration [mean (SD)] | 13.6 (7.6) | 12.9 (7.4) | 13.7 (7.7) | 0.740 |
| Dementia [*N* (%)] | 33 (58.9) | 5 (50.0) | 28 (60.9) | 0.725 |
| Brain weight [g, mean (SD)] | 1,303 (113) | 1,343 (135) | 1,297 (109) | 0.540 |
| Argyrophilic grain [*N* (%)] | 2 (3.6) | 0 (0.0) | 2 (4.3) | 1.000 |
| Hippocampal sclerosis [*N* (%)] | 0 (0.0) | 0 (0.0) | 0 (0.0) | 1.000 |
| Clinical diagnosis | | | | |
| Parkinson's disease | 29 (51.8) | 7 (70.0) | 22 (47.8) | 0.299 |
| Parkinson's disease with dementia[b] | 23 (41.1) | 2 (20.0) | 21(45.7) | 0.172 |
| Dementia with Lewy bodies | 4 (7.1) | 1 (10.0) | 3 (6.5) | 1.000 |
| Lewy body type pathology [27] | | | | |
| Brain stem type | 10 (17.9) | 2 (20.0) | 8 (17.4) | 1.000 |
| Limbic type | 29 (51.8) | 2 (20.0) | 27 (58.7) | 0.038[c] |
| Diffuse neocortical type | 17 (30.4) | 6 (60.0) | 11 (23.9) | 0.052[c] |
| Braak NFT stage [4] | | | | |
| Stages 0–II | 37 (66.1) | 7 (70.0) | 30 (65.2) | 1.000 |
| Stages III–IV | 14 (25.0) | 2 (20.0) | 13 (28.3) | 0.713 |
| Stages V–VI | 5 (8.9) | 1 (10.0) | 3 (6.5) | 1.000 |
| DLB likelihood [27][d] | | | | |
| Low | 10 (17.9) | 2 (20.0) | 8 (17.4) | 1.000 |
| Intermediate | 15 (26.8) | 2 (20.0) | 13 (28.3) | 0.713 |
| High | 31 (55.4) | 6 (60.0) | 25 (54.3) | 1.000 |

[a] TDP-43-positive LBD cases versus TDP-43-negative LBD cases

[b] The clinical diagnosis of Parkinson's disease with dementia was based on motor impairment preceded by at least 1 year [27]

[c] Although not significant, the frequency of limbic type of LBD pathology was higher in TDP-43-negative cases, while the frequency of diffuse neocortical type LBD was higher in TDP-43-positive cases

[d] The likelihood that Lewy body related pathology is associated with a DLB clinical syndrome

pS409/410, rabbit, polyclonal, 1:1,000 [13]), phosphorylated tau (AT8, mouse, monoclonal, 1:3,000, Innogenetics, Ghent, Belgium), phosphorylated α-synuclein (#1175, rabbit, polyclonal, 1:1,000, [30]), and Aβ (4G8, mouse, monoclonal, 1:2,000, Covance Research Products Inc., Dedham, MA). Deparaffinized sections were incubated with 1% $H_2O_2$ in methanol for 20 min to eliminate endogenous peroxidase activity. When using anti-α-synuclein and anti-TDP-43 antibodies, sections were pretreated in a microwave oven for 5 min in 10 mM sodium citrate buffer, pH 6.0, at 100°C to enhance immunoreaction. For Aβ immunostaining, sections were incubated in 95% formic acid for 5 min. No pretreatment was performed for AT8 immunostaining. After blocking with 10% normal serum, sections were incubated for 1 h at room temperature with one of the primary antibodies. After three 5-min washes in PBS, sections were incubated in biotinylated secondary antibody for 30 min, and then in avidin–biotinylated horseradish peroxidase complex (ABC Elite kit, Vector, Burlingame, CA, USA) for 30 min. The peroxidase labeling was visualized with 0.2% 3,3′-diaminobenzidine (DAB) as chromogen. Sections were lightly counterstained with hematoxylin.

Semiquantitative assessment

TDP-43, α-synuclein, tau, and Aβ pathologies in the amygdala, anterior and posterior portions of the entorhinal cortex, hippocampal dentate gyrus, CA1, 2, 3, and 4 regions, subiculum, fusiform gyrus, and occipitotemporal gyrus were semiquantitatively evaluated using the following grading system blinded to any clinical or pathological information:

(a) The total number of TDP-43-positive neuronal cytoplasmic inclusions (NCIs) in each anatomical region was assessed as follows: −, no lesion; +, one inclusion; ++, two or three inclusions; +++, four or five inclusions; ++++, 6–10 inclusions; +++++, 11 or over inclusions. The topographic distribution of TDP-43 pathological changes was assessed using the following system, which was similar to that reported by Amador-Ortiz et al. [1]—the amygdala type: inclusions were present only in the amygdala; the limbic type: inclusions extend to the amygdala, hippocampal dentate gyrus, CA1-4, entorhinal cortex, and fusiform gyrus, but not in the occipitotemporal

gyrus; the temporal type: inclusions are present in the limbic system and also in the occipitotemporal gyrus.

(b) The LBD cases were classified, irrespective of the presence or absence of dementia, into brain stem-predominant type, limbic type, and diffuse neocortical type, according to the distribution of α-synuclein pathology as recommended by the Third Consensus Guideline for DLB [27]. In addition, the severity of α-synuclein pathology in the substantia nigra, amygdala, and temporal cortex was semiquantitatively assessed at ×100 magnification using the following method, again fundamentally consistent with protocols of the Third Consensus Guideline for DLB [27]: grade 1, one Lewy body (LB) or Lewy neurites (LNs) per few fields; grade 2, one to three LBs and sparse LNs per one field; grade 3, four to ten LBs and scattered LNs per one field; grade 4, over 11 LBs and LNs per one field.

(c) Tau-positive neuronal inclusions were counted at ×100 magnification: 0, no tau-positive lesions; 1, one neuronal inclusion per few microscopic fields; 2, one to three inclusions in every field; 3, 4–30 inclusions in every field; 4, over 30 inclusions associated with numerous neurites in every field. The distribution of tau pathology in LBD cases was assessed according to Braak NFT stage on AT8 immunostained sections [4].

(d) Aβ deposits were counted at ×100 magnification: 0, no Aβ deposits; 1, two to three Aβ plaques in each field; 2, 4–10 Aβ plaques in each field; 3, 11–20 Aβ plaques in each field; 4, more than 20 Aβ deposits in each field.

Hippocampal sclerosis (HS) was defined by neuronal loss with gliosis in the hippocampal CA1 and/or subiculum, with relatively preserved neurons in CA2, 3, and 4 regions and absence of intracellular and extracellular NFTs, or ischemic changes that might explain neuronal loss in the CA1 and subiculum. HS was assessed on hematoxylin–eosin stained sections blind to any clinical or pathological information.

### Statistical analysis

The Mann–Whitney *U* test and Fisher's exact test were used to compare the demographic and pathological data between two groups. Correlations between (a) the rating of TDP-43 pathology in the amygdala and clinical variables, (b) the rating of TDP-43 pathology and that of α-synuclein, tau, or Aβ pathology in each anatomical region, and (c) the rating of TDP-43 pathology in the amygdala and that of α-synuclein or tau pathology in each region were assessed by Spearman's rank-order correlation test. Multiple logistic regression models were used to assess the influence of predictor variables (age at death, the severities of tau and α-synuclein pathologies) on the occurrence of TDP-43 pathology. The effects were described as odds ratios and 95% confidence interval (CI). Statistical analysis was performed using Excel, Stat View version J-4.5, and SPSS 10.0J. A $P$ value $<0.05$ was accepted as significant; however, in analyses of comparisons between two groups and correlations between two variables, a $P$ value $<0.01$ was accepted as significant to interpret the results with caution because multiple tests have been done.

### Confocal laser scanning microscopy

Double-labeling immunofluorescence was performed with the combination of (a) phosphorylation-dependent rabbit polyclonal anti-TDP-43 (pAb pS409/410, 1:1,200 [13]) and anti-tau antibodies (AT8, mouse, monoclonal, 1:500, Innogenetics, Ghent, Belgium), and (b) phosphorylation-dependent mouse monoclonal anti-TDP-43 (mAb pS409/410, 1:1,200 [16]) and phosphorylation-dependent anti-α-synuclein antibodies (#1175, rabbit, polyclonal, 1:1,000, [30]). Sections from the amygdala in LBD cases with TDP-43 pathology were pretreated by heating in a microwave oven for 5 min in 10 mM sodium citrate buffer, pH 6.0, at 100°C, allowed to cool then permeabilized with 0.2% (v/v) Triton X-100 in phosphate buffered saline (PBS). Following washing in PBS, non-specific antibody binding was blocked with normal sera and sections were incubated with a mixture of the two primary antibodies for 1 h at room temperature. After washing in PBS, sections were incubated with fluorescence-labeled secondary antibodies [AlexaFluor 488 anti-rabbit IgG (1:200) and AlexaFluor 555 anti-mouse IgG (1:200), Molecular Probes, Invitrogen, Paisley, UK]. After washing with PBS, sections were incubated with Toto-3 Iodide (Molecular Probes, Invitrogen, Paisley, UK) with 1 mg/ml RNase (Roche Diagnostics GmbH, Manheim, Germany) at 37°C. To quench (lipofuscin) autofluorescence, sections were incubated in 0.1% Sudan Black B for 10 min at room temperature and washed with 0.1% Triton X-PBS for 30 min. Sections were coverslipped with Vectashield mounting media (Vector Laboratories Inc., Burlingame, CA). Images were collected on a Leica TCS SP5 AOBS upright confocal (Leica Microsystems, Milton Keynes, UK) using the 488 nm (19%), 543 nm (30%) and 633 nm (60%) laser lines. To eliminate cross-talk between channels, the images were collected sequentially.

### Immunoblotting

Frozen tissues from the amygdala, hippocampus, and frontal and temporal cortex from two LBD cases (one TDP-43-positive and one TDP-43-negative case), one FTLD-TDP case as a positive control, and one pathologically normal control case were prepared for western blotting according to

methods previously described by Neumann et al. [29]. Briefly, fresh frozen brain was homogenized in low salt (LS) buffer containing 10 mM Tris pH 7.5, 5 mM EDTA pH 8.0, 1 mM DTT, 10% (w/v) sucrose and Roche complete EDTA free protease inhibitor. Homogenates were sequentially extracted with increasing strength buffers [Triton X-100 buffer (LS buffer + 1% Triton X-100 + 0.5 M NaCl), Triton X-100 buffer with 30% sucrose to float myelin, Sarkosyl buffer (LS buffer + 1% *N*-lauroyl-sarcosine + 0.5 M NaCl)]. Detergent insoluble pellets were extracted in 0.25 ml/g urea buffer (7 M urea, 2 M thiourea, 4% 3-[(3-cholamidopropyl)dimethylammonio]-1-propanesulfonate (CHAPS), 30 mM Tris–HCl pH 8.5, Roche complete EDTA free protease inhibitor). Prior to SDS-PAGE immunoblot analysis, urea fractions were added in 1:1 ratio to SDS sample buffer (10 mM Tris pH 6.8, 1 mM EDTA, pH 8.0, 40 mM DTT, 1% SDS, 10% sucrose, 0.01% bromophenol blue). Protein was resolved on 12% Tris–glycine SDS-PAGE gels along with size standard (Bio-Rad kaleidoscope broad-range marker; BioRad, Hercules, CA). Proteins were transferred onto nitrocellulose membrane (Hybond ECL, GE Life Sciences, UK) and blocked overnight at 4°C in 5% (w/v) milk solution [5% powdered milk in Tris-buffered saline containing 0.1% Tween-20 (TBS-T)]. Membranes were incubated in phosphorylation-dependent mouse monoclonal antibody (mAb pS409/410, mouse, 1:1,000 [16]) for 1 h at room temperature followed by HRP-conjugated goat anti-mouse secondary antibody (Santa Cruz Biotechnology Inc, CA). Antibodies were visualized by incubating in enhanced chemiluminescent reagent (ECL, GE Life Sciences) and imaged using the ImageQuant 350 system fitted with a F0,95 25 mm Fixed Lens (GE Healthcare, Life Sciences, UK). TDP-43-probed membranes were exposed for 5 min at different timeframes to obtain multiple images of differing intensity. Images were processed using ImageQuant TL software (GE Healthcare, Life Sciences, UK).

## Results

### Frequency and distribution of TDP-43 pathology in all LBD cases

Of the 56 LBD cases, 10 (17.9%) had TDP-43-positive neuronal intracytoplasmic inclusions (NCIs) (Table 1). The amygdala (all 10 TDP-43 positive cases) was most frequently affected by TDP-43 pathology, followed by the anterior portion of the entorhinal cortex (7/10 cases), hippocampal dentate gyrus (3 cases), subiculum (3 cases), and CA1, fusiform gyrus, and occipitotemporal gyrus (2 cases for each) (Table 2; Fig. 1). The distribution of TDP-43 pathology was the amygdala type in one case, the limbic type in seven cases, and the temporal type in two cases. No neuronal intranuclear inclusions were noted in any LBD case.

### α-Synuclein and tau pathologies in LBD cases with and without TDP-43 pathology

Clinical and pathological features in those LBD cases with and without TDP-43 pathology are shown in Table 1. There was no statistically significant difference in the sex ratio, mean age at onset, age at death, disease duration, or frequency of dementia between these two groups. There was no significant correlation between demographic variables and the rating of TDP-43 pathology in the amygdala. None of our LBD cases, including TDP-43-positive cases, had significant neuronal loss in the hippocampal CA1 or subiculum consistent with the definition of HS.

α-Synuclein pathology in the 10 TDP-43-positive cases was more widely distributed than that in TDP-43-negative cases. The diffuse neocortical type of LBD was the most common pathological subtype in the TDP-43-positive cases (six cases), followed by limbic type and brainstem-predominant type (two cases each) (Fig. 2a). In contrast, in the TDP-43-negative LBD cases, the limbic type was most frequent (58.7%), while only 23.9% cases had diffuse neocortical type (Fig. 2a). The frequency of diffuse neocortical type cases in the TDP-43-positive cases tended to be higher than that in the TDP-43-negative cases (Mann–Whitney $U$ test, $P = 0.052$). Consistent with these results, was the observation that the rating of α-synuclein pathology in the temporal cortex in the TDP-43-positive cases was significantly more severe than that in the TDP-43-negative cases (Mann–Whitney $U$ test, $P = 0.003$; Fig. 2b). There was no significant difference in the rating of α-synuclein pathology, in either the substantia nigra or the amygdala, between the TDP-43-positive and TDP-43-negative cases. The Spearman rank correlation coefficient showed a moderate correlation between the ratings for α-synuclein pathology in the temporal cortex and TDP-43 pathology in the amygdala (Spearman rho = 0.398, $P < 0.01$). In any other regions, there was no significant correlation between the ratings for TDP-43 and α-synuclein pathologies, and Spearman rho ranged from −0.087 to 0.122.

The ratings for tau pathology in the hippocampal dentate gyrus in the TDP-43-positive cases tended to be higher than those in the TDP-43-negative cases (Mann–Whitney $U$ test, $P = 0.037$). Likewise, although not significantly, Braak NFT stage in the TDP-43-positive cases also tended to be higher than that in the TDP-43-negative cases (Fig. 3). Although not significant, a moderate correlation was observed between the ratings for tau pathology in the hippocampal dentate gyrus and those for TDP-43

**Table 2** Distribution of TDP-43 pathology in LBD cases

| No. | TDP-43 pathology | | | | | | | | | | | Hippocampal sclerosis | Braak NFT stage | Argyrophilic grains | DLB pathology subtype | DLB likelihood | Clinical diagnosis |
|---|---|---|---|---|---|---|---|---|---|---|---|---|---|---|---|---|---|
| | Amygdala | ant.EC | DG | CA3/4 | CA2 | CA1 | SB | post.EC | FG | OTG | Distribution | | | | | | |
| *LBD-Ltau cases* | | | | | | | | | | | | | | | | | |
| 1 | + | − | − | − | − | − | − | − | − | − | Amygdala | − | I | − | Brain stem | Low | PD |
| 2 | + | + | − | − | − | − | − | − | − | − | Limbic | − | I | − | Limbic | High | PD |
| 3 | +++ | +++++ | − | − | − | − | − | − | − | − | Limbic | − | II | − | Diffuse | High | PD |
| 4 | ++ | + | − | − | − | + | ++ | − | − | − | Limbic | − | II | − | Diffuse | High | PDD |
| 5 | +++++ | + | + | − | − | − | − | + | − | − | Limbic | − | II | − | Diffuse | High | PD |
| 6 | ++++ | ++ | ++ | − | − | − | − | − | + | + | Temporal | − | I | − | Limbic | High | PDD |
| 7 | +++++ | +++++ | − | − | − | + | ++ | − | + | ++ | Temporal | − | II | − | Diffuse | High | DLB |
| % | 100.0 | 85.7 | 28.6 | 0.0 | 0.0 | 28.6 | 28.6 | 14.3 | 28.6 | 28.6 | | | | | | | |
| *LBD-Htau cases* | | | | | | | | | | | | | | | | | |
| 8 | ++ | − | + | − | − | − | − | − | − | − | Limbic | − | III | − | Brain stem | Low | PD |
| 9 | +++ | + | − | − | − | − | − | − | − | − | Limbic | − | V | − | Diffuse | Intermediate | PD |
| 10 | ++++ | − | − | − | − | − | +++ | − | − | − | Limbic | − | VI | − | Diffuse | Intermediate | PD |
| % | 100 | 33.3 | 33.3 | 0.0 | 0.0 | 0.0 | 33.3 | 0.0 | 0.0 | 0.0 | | | | | | | |

*LBD-Ltau* LBD with no or low tau burden of Braak NFT stages 0–II, *LBD-Htau* LBD with high tau burden of Braak NFT stages III–VI, *ant.EC* the anterior portion of the entorhinal cortex, *DG* hippocampal dentate gyrus, *SB* subiculum, *post.EC* posterior portion of the entorhinal cortex, *FG* fusiform gyrus, *OTG* occipitotemporal gyrus, *PD* Parkinson's disease, *PDD* Parkinson's disease with dementia, *DLB* dementia with Lewy bodies

DLB pathology subtype [27]: *brain stem* brain stem-predominant type, *limbic* limbic type, *diffuse* diffuse neocortical type

The stages of TDP-43 pathology: −, no lesion in the anatomical region; +, one inclusion in the anatomical region; ++, two to three inclusions in the anatomical region; +++, four to five inclusion in the anatomical region; ++++, 6–10 inclusions in the anatomical region; +++++, 11 or over inclusions in the anatomical region. The distribution of TDP-43 pathology, amygdala, amygdala type, limbic, limbic type, temporal, temporal type

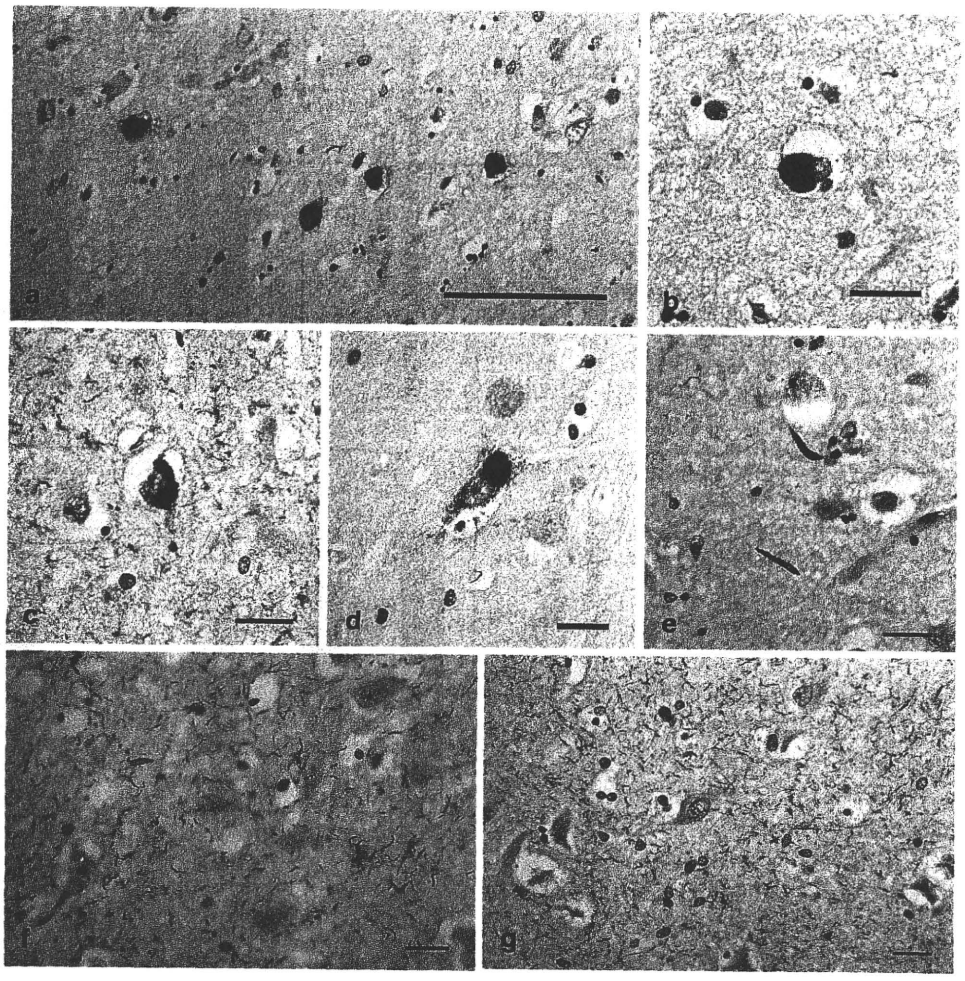

**Fig. 1** Phosphorylated TDP-43 pathology in LBD-Ltau cases. TDP-43-positive NCIs in the entorhinal cortex (**a**), amygdala (**b, c**), and CA1 (**d**). TDP-43-positive dystrophic neurites are also scattered in the amygdala (**e**). In some cases, abundant fine and short threads-like structures are also seen in the CA1 to subiculum (**f, g**). pAb pS409/410 immunohistochemistry. **a, c, d, g** Diffuse neocortical type LBD-Ltau cases (Braak NFT stage II), **b, e, f** limbic type LBD-Ltau cases (Braak NFT stage I). *Scale bars* **a** 100 μm, **b–g** 20 μm

pathology in the amygdala (Spearman rho = 0.301, $P < 0.05$). In any other regions, there was no significant correlation between the ratings for TDP-43 and tau pathologies, and Spearman rho ranged from −0.092 to 0.178.

Ratings for Aβ pathology were not significantly different between the TDP-43-positive and TDP-43-negative LBD cases. Spearman correlation coefficients did not indicate any significant correlation between the severities of Aβ and TDP-43 pathologies in any region, and Spearman rho ranged from 0.103 to 0.227.

## Relationship between α-synuclein and TDP-43 pathologies in LBD-Ltau and LBD-Htau cases

The relationship between α-synuclein and TDP-43 pathologies in LBD-Ltau (Braak NFT stages 0–II) and LBD-Htau cases (Braak NFT stages III–VI) was examined separately. The sex ratio, mean age at onset, age at death, disease duration, frequency of dementia were not significantly different between the TDP-43-positive and TDP-43-negative cases in the LBD-Ltau cases, as well as in the LBD-Htau cases (Table 3).

In the LBD-Ltau cases with TDP-43 pathology, the most frequent LBD subtype was the diffuse neocortical type (57.1%), followed by limbic (28.6%) and brain stem-predominant (14.3%) types (Fig. 4). In contrast, in LBD-Ltau cases without TDP-43 pathology, the limbic type was most frequent (56.7%), while the diffuse neocortical type was seen in only 23.3% cases and brain stem-predominant type in 20.0%. In the LBD-Ltau group, the rating of α-synuclein pathology in the temporal cortex in the TDP-43-positive cases tended to be higher than that in the TDP-43-negative cases (Mann–Whitney $U$ test, $P = 0.042$). Although case numbers were small, a similar trend was seen in the LBD-Htau cases: 2 of 3 TDP-43-positive LBD cases were diffuse neocortical type, while only 4 of 16 TDP-43-negative cases were this subtype (67 vs. 25%).

Both in LBD-Ltau or in LBD-Htau cases, the ratings for tau and Aβ pathologies were not significantly different between TDP-43-positive and TDP-43-negative cases, in any region.

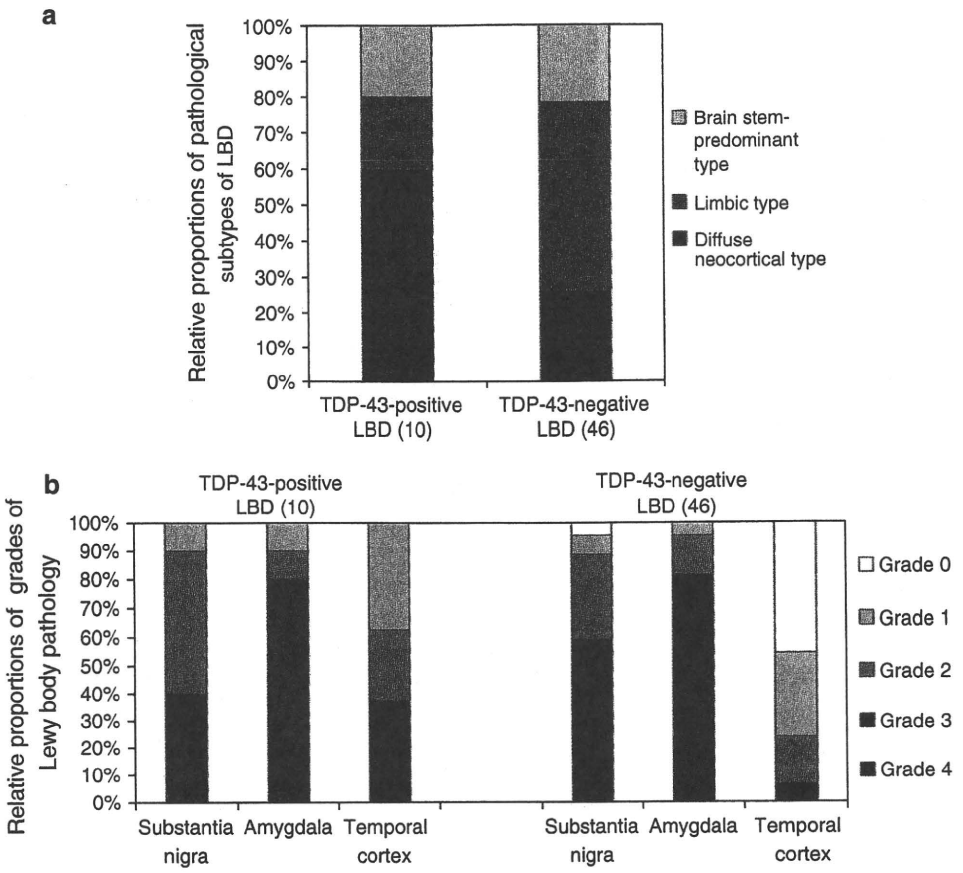


**Fig. 2** α-Synuclein pathology in all LBD cases with and without TDP-43 pathology. **a** The distribution of pathological subtypes of LBD in TDP-43-positive and TDP-43-negative groups. The frequency of diffuse neocortical type in TDP-43-positive LBD cases tends to be higher than that in TDP-43-negative LBD cases ($P = 0.052$). The number of cases in each group is shown in *brackets*. **b** The rating of α-synuclein pathology in TDP-43-positive and TDP-43-negative LBD cases. α-Synuclein pathology in the temporal cortex in TDP-43-positive cases was significantly more severe than that in TDP-43-negative cases ($P = 0.003$)

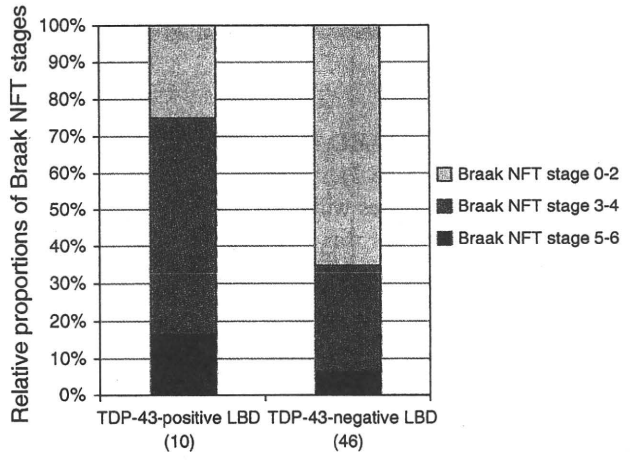


**Fig. 3** Braak NFT stage in LBD cases with and without TDP-43 pathology. Tau pathology in TDP-43-positive LBD cases tended to be more severe than that in TDP-43-negative LBD cases. The number of cases in each group is shown in *brackets*

## Frequency of TDP-43 pathology by clinical and pathological subtypes of LBD

There was no clear relationship between the occurrence of TDP-43 pathology and clinical phenotypes of LBD in our series: TDP-43 pathology was found in 7 of 29 PD cases (24.1%), 2 of 23 PDD cases (8.7%), and 1 of 4 DLB cases (25%). The overall frequency of TDP-43 pathology was 11.1% in LBD cases with dementia and 24.1% in LBD cases without it. However, in LBD-Ltau cases (Braak NFT stages 0–II), the duration from disease onset to the development of dementia in TDP-43-positive cases tended to be shorter than that in TDP-43-negative cases ($2.0 \pm 1.7$ vs. $11.9 \pm 7.0$ years, $P = 0.046$, Mann–Whitney $U$ test).

In contrast to clinical phenotypes, there was a trend for TDP-43 pathology to be more frequently present in cases with severe α-synuclein pathology. In LBD-Ltau cases, TDP-43 pathology was noted in 4 of 11 diffuse neocortical type LBD-Ltau cases (36.4%), whereas it was only present in 2 of 19 cases of limbic type LBD (10.5%) and in 1 of 17 brain stem-predominant type LBD (14.3%) cases. In LBD-Htau cases, 2 of the 5 diffuse neocortical type cases with severe tau pathology (Braak NFT stages V–VI) also had TDP-43 pathology. The overall frequency of TDP-43 pathology in diffuse neocortical type LBD cases was 35.3% (6 of 17 cases).

## Effects of α-synuclein and tau pathologies on development of TDP-43 pathology

A multiple logistic regression model was used to evaluate whether pathological subtypes of LBD, Braak NFT stage,

**Table 3** Clinical and pathological features in LBD-Ltau and LBD-Htau cases

| | LBD-Ltau (Braak NFT stages 0–II) | | | | LBD-Htau (Braak NFT stages III–VI) | | | |
|---|---|---|---|---|---|---|---|---|
| | All | TDP-43-positive | TDP-43-negative | *P* value[a] | All | TDP-43-positive | TDP-43-negative | *P* value[b] |
| *N* (%) | 37 (66.1)[c] | 7 (18.9) | 30 (81.1) | – | 19 (33.9)[c] | 3 (15.8) | 16 (84.2) | – |
| Male [*N* (%)] | 29 (78.4) | 6 (85.7) | 23 (76.7) | 0.677 | 13 (68.4) | 2 (66.7) | 11 (68.8) | 1.000 |
| Age at onset [mean (SD)] | 60.9 (15.2) | 65.1 (13.1) | 59.9 (15.7) | 0.455 | 66.3 (7.4) | 65.3 (4.7) | 66.5 (7.9) | 0.958 |
| Age at death [mean (SD)] | 76.1 (7.9) | 75.7 (7.2) | 76.2 (8.2) | 0.732 | 78.4 (5.2) | 81.3 (3.2) | 77.9 (5.4) | 0.360 |
| Duration [mean (SD)] | 14.3 (7.7) | 11.5 (8.4) | 14.9 (7.6) | 0.179 | 12.3 (7.5) | 15.7 (4.9) | 11.6 (7.8) | 0.360 |
| Dementia [*N* (%)] | 23 (62.2) | 5 (71.4) | 18 (60.0) | 0.687 | 10 (52.5) | 0 (0.0) | 10 (62.5) | 0.059 |
| Brain weight [g, mean (SD)] | 1,290 (103) | 1,299 (132) | 1,289 (102) | 1.000 | 1,327 (129) | 1,387 (151) | 1,312 (125) | 0.368 |
| Argyrophilic grain [*N* (%)] | 0 (0.0) | 0 (0.0) | 0 (0.0) | 1.000 | 2 (10.5) | 0 (0.0) | 2 (12.5) | 1.000 |

*LBD-Ltau* LBD with no or low tau burden of Braak NFT stages 0–II [4], *LBD-Htau* LBD with high tau burden of Braak NFT stages III–VI

[a] TDP-43-positive LBD-Ltau cases versus TDP-43-negative LBD-Ltau cases

[b] TDP-43-positive LBD-Htau cases versus TDP-43-negative LBD-Htau cases

[c] The proportion to all LBD cases

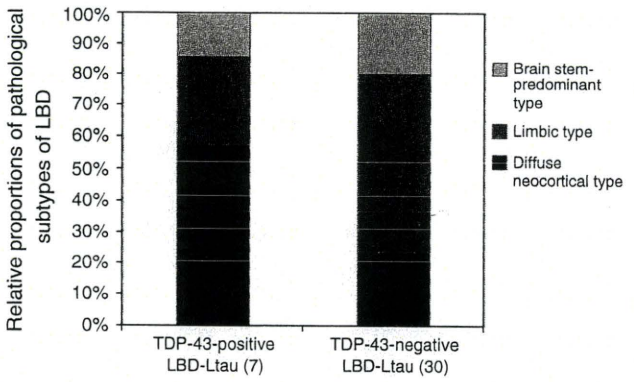


**Fig. 4** Distribution of LBD subtypes in LBD-Ltau cases (Braak NFT stages 0–II). Diffuse neocortical type in TDP-43-positive cases was more frequent than that in TDP-43-negative cases. The number of cases in each group is shown in *brackets*

and age at death could be used as possible predictors for the development of TDP-43 pathology. After combining categories in which the number of cases was small (Braak NFT stages 0–II or Braak NFT stages III–VI) and pathological subtype of LBD (diffuse neocortical type or others) data were submitted as binary variables into the model. The presence of diffuse neocortical type of LBD was the only significant independent predictor of the development of TDP-43 pathology (odds ratio 7.6, 95% CI 1.46–39.1, $P = 0.016$).

Multiple logistic regression analysis was also used to examine whether the ratings of the severities of α-synuclein and tau pathologies in the amygdala and age at death were predictors of the development of TDP-43 pathology. Again, after combining categories in which the number of cases was small, the ratings of α-synuclein (grades 1–3 or grade 4) and tau pathologies (Braak NFT stages 0–II or Braak NFT stages III–IV) were submitted as binary variables into the model. However, neither of these variables predicted the development of TDP-43 pathology, although the odds ratio of severe α-synuclein pathology in the amygdala was high (odds ratio 3.5, 95% CI 0.71–17.1, $P = 0.122$).

## Double-labeling confocal microscopy of phosphorylated TDP-43, tau, and α-synuclein

In the amygdala, TDP-43 accumulation was often colocalized with α-synuclein accumulation in NCIs and dystrophic neurites (Fig. 5a–i). TDP-43 was also often colocalized with tau labeling (Fig. 5j–o), but there were also some TDP-43-positive α-synuclein-negative lesions (Fig. 5d–i) and TDP-43-positive tau-negative lesions (Fig. 5j–l). In the hippocampal granular cells, TDP-43 and tau were only rarely colocalized (data not shown).

## Biochemical analysis of TDP-43 in LBD cases

Immunoblot analysis of the sarkosyl-insoluble urea-soluble fraction using mAb pS409/410 in LBD cases with TDP-43 pathology demonstrated distinct bands at approximately 45 and 25 kDa, as well as high molecular weight (HMW) smears (Fig. 6, lanes 3 and 4) similar to those seen in the FTLD-TDP case (lane 6). These pathological bands and the HMW smear were not seen in the LBD cases without TDP-43 pathology (lanes 1 and 2) or in the normal control cases (lane 5).

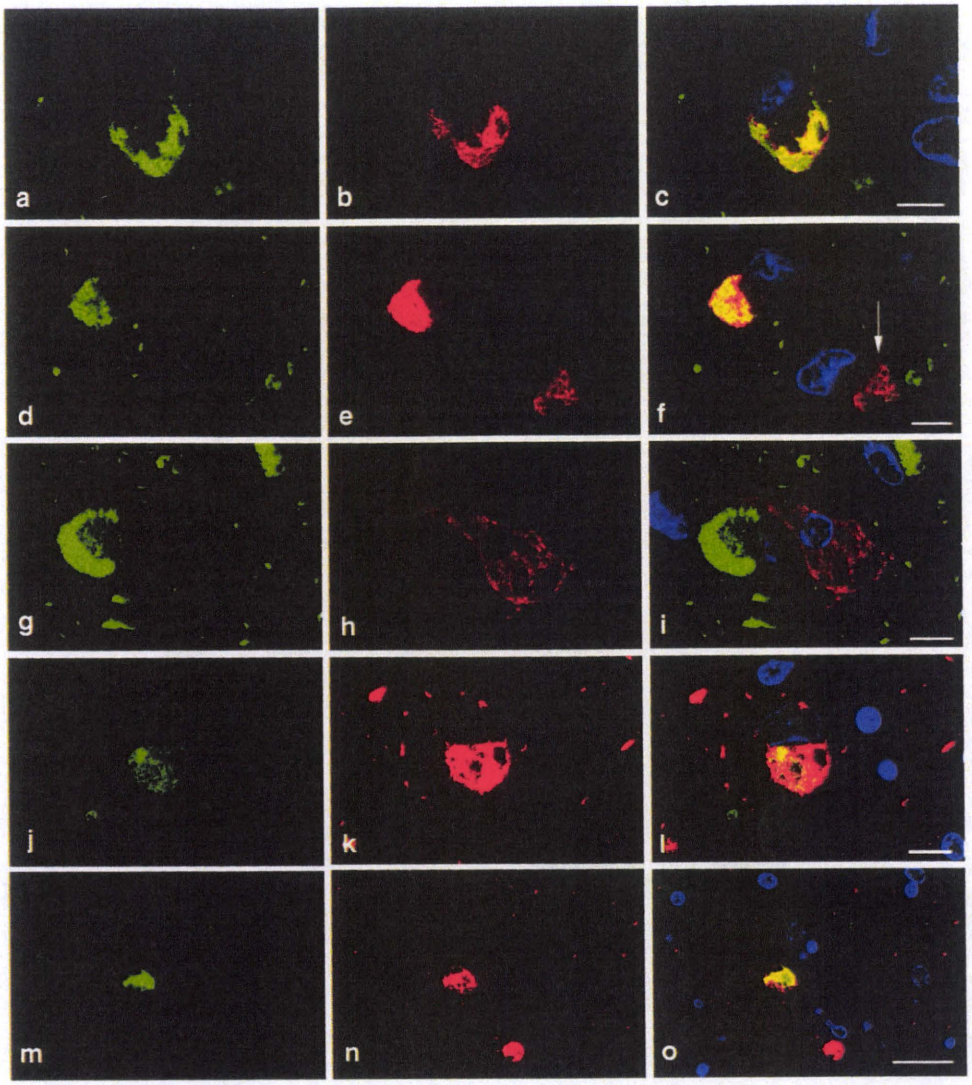


**Fig. 5** Confocal double immunofluorescence of the combination of α-synuclein (**a**, **d**, **g**) and TDP-43 (**b**, **e**, **h**), and the combination of TDP-43 (**j**, **m**) and tau (**k**, **n**) in the amygdala in LBD cases. Blue fluorescence in merged images (**c**, **f**, **i**, **l**, **o**) are nuclei. **a–c** TDP-43 (*red*) is colocalized with α-synuclein (*green*) in an inclusion. **d–f** In a left inclusion, α-synuclein (*green*) is colocalized with TDP-43 (*red*). However, the right TDP-43-positive inclusion (*arrow*) shows only faint α-synuclein immunolabeling (*green*). **g–i** A left horseshoe-shaped inclusion is stained only with an α-synuclein antibody, while a right neuron shows diffuse cytoplasmic TDP-43 labeling (*red*) without α-synuclein immunoreactivity. **j–o** TDP-43 (*green*) is often colocalized with tau labeling (*red*) in cytoplasmic inclusions. There are a few TDP-43-positive tau-negative lesions (**l**, *green*). **a–i** #1175 and mAb pS409/410 double immunofluorescence in a LBD-Ltau case (Braak NFT stage II), **j–o** pAb pS409/410 and AT8 double immunofluorescence in a LBD-Htau case (Braak NFT stage VI). *Scale bars* **a–c** 7.5 μm, **d–f** 7.5 μm, **g–i** 7.5 μm, **j–l** 10 μm, **m–o** 25 μm

## Discussion

This is the first study demonstrating a high frequency of TDP-43 pathology in LBD-Ltau cases (Braak NFT stages 0–II). The overall frequency of TDP-43 pathology was 19%, and the frequency of TDP-43 pathology in diffuse neocortical type LBD cases was as much as 36%, which was higher than those in other LBD subtypes (11–14%). In all LBD cases in this study, even in LBD-Ltau cases, the proportion of diffuse neocortical type LBD cases among the TDP-43-positive cases was approximately 1.5 times higher than that in the TDP-43-negative cases, and multivariate analysis demonstrated that severe α-synuclein pathology was a predictor of TDP-43 accumulation in LBD independent of age at death and tau pathology. Double immunofluorescence demonstrated that TDP-43 was often colocalized with α-synuclein or tau in the amygdala. These findings suggest that α-synuclein may play some role in the process associated with the development of TDP-43 pathology in LBD cases.

Previous data regarding TDP-43 accumulation in LBD cases are limited. In an early study by Nakashima-Yasuda et al. [28], the overall frequency of TDP-43 pathology in LBD cases was reported to be 18.9%. This frequency appears to be similar to that in all LBD cases examined in our study (17.9%), even though these authors employed a 'conventional' phosphorylation-independent TDP-43 antibody. However, these frequencies cannot be directly compared, because the pathological backgrounds between two LBD series may be different. For example, the degree of tau pathology in the Nakashima-Yasuda series tended to be more severe than that in the present series: the proportion of LBD cases having severe tau pathology (Braak NFT stages V–VI) being 21% (38 of 180 LBD cases), far higher than that in our LBD series (8.9%). Conversely, the proportion of cases of Braak NFT stages 0–II in the

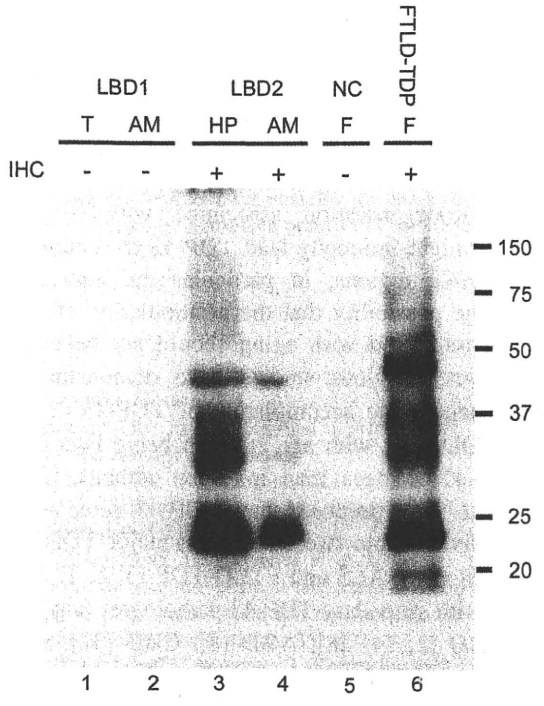


**Fig. 6** Immunoblot analysis of the sarkosyl-insoluble fraction in representative LBD cases with phosphorylation-dependent monoclonal anti-TDP-43 antibody (mAb pS409/410). The approximately 45 and 25 kDa fragments, as well as smears are strongly labeled in a LBD case with TDP-43 pathology (*lanes 3* and *4*) and a FTLD-TDP case (*lane 6*). These 45 and 25 kDa bands and smears were not labeled in any other cases without detectable TDP-43 pathology by immunohistochemistry (*lanes 1*, *2*, and *5*). Normal 43 kDa TDP-43 is not stained by this phosphorylation-dependent antibody in any cases. *LBD* Lewy body disease, *NC* normal control, *AM* amygdala, *HP* hippocampus, *F* frontal cortex, *T* temporal cortex, *IHC* pAb pS409/410 immunohistochemistry

Nakashima-Yasuda series was about 50% (91 of 180 LBD cases), this being smaller than that in our series (66.1%). Considering that several studies have suggested a possible relationship between TDP-43 accumulation and the severity of tau pathology in several tauopathies [2, 8, 28], it is plausible that the differences regarding the degree of tau pathology might have influenced the overall frequency of TDP-43 pathology in LBD series. More recently, Arai et al. [2], using the same phosphorylation-dependent TDP-43 antibody employed in the present study, reported TDP-43 pathology in up to 56% of DLB and DLB + AD cases. Although Arai et al. did not present detailed data regarding tau and α-synuclein pathologies, the degree of tau pathology, at least, in their TDP-43-positive LBD cases tended to be more severe than that in our TDP-43-positive cases: 43% of their TDP-43-positive LBD cases was classified as having severe tau pathology of Braak NFT stages V–VI (compared to 20% in the present TDP-43-positive cases). Because of the relative paucity of cases having severe tau pathology of Braak NFT stages V–VI in our series (2 of 5 cases, 40%), it is difficult to discuss about the significance of the frequency of TDP-43 pathology in this subpopulation of LBD cases. However, similar frequencies have been observed in some subgroups in Nakashima-Yasuda et al. [28] series where the pathological background may be similar to that in our series. These authors reported that TDP-43 pathology in 47% of LBD cases of Braak NFT stages V–VI (the severity of α-synuclein pathology in this group was not shown), and in 31% of DLB + AD cases (a high and intermediate likelihood for both DLB and AD pathology [27, 31]). We could not fully examine the differences of the severity and distribution of TDP-43 pathology between diffuse neocortical type of LBD cases with and without severe tau pathology, because the number of cases having severe tau pathology was small. The data regarding the difference of TDP-43 pathology between these two groups, including the presence or absence of TDP-43 accumulation in the frontal and occipital cortices, may provide clues to understand the impacts of not only α-synuclein but also tau accumulations on TDP-43 accumulation in LBD cases.

Whereas the degree of α-synuclein pathology is highly variable among LBD cases, there was few previous data available regarding the relationship between the severity of α-synuclein pathology and the development of TDP-43 pathology. In the light of present results, the severity of α-synuclein pathology may be a potential factor for the development of TDP-43 pathology. We suggest that the severity of α-synuclein pathology should be considered when interpreting the frequency of TDP-43 pathology in LBD cases, and probably, in other pathological conditions as well. It is notable that TDP-43 pathology was frequently found in our LBD cases even when severe tau pathology did not coexist, especially in cases of the diffuse neocortical type. Although inconsistent with findings of an early study in which none of ten LBD-Ltau cases had TDP-43 pathology [28], Higashi et al. [14] reported TDP-43 pathology in 3/7 LBD-Ltau cases using a phosphorylation-independent antibody and Arai et al. [2] reported that all of four LBD-Ltau cases in their series had variable degrees of TDP-43 pathology. Our present results agree with these findings and suggest a possible association of α-synuclein and TDP-43 accumulations in LBD-Ltau cases.

On the other hand, in a study by Josephs et al. [20] in which 84 AD cases were examined, multivariate analysis did not demonstrate any significant effect of the presence of α-synuclein pathology on the development of TDP-43 accumulation in AD. In their AD series, although the prevalence of α-synuclein pathology was only 25%, the frequency of α-synuclein pathology in TDP-43-positive cases was significantly higher than in TDP-43-negative cases (38 vs. 18%). No detailed data about the degree of α-synuclein pathology in this series was presented. In the